Journal Pre-proof

Novel NO-releasing scopoletin derivatives induce cell death via mitochondrial apoptosis pathway and cell cycle arrest

Zhixian Shi, Na Li, Cheng Chen, Yujin Wang, Zhichao Lei, Li Chen, Jianbo Sun

PII: S0223-5234(20)30356-1

DOI: https://doi.org/10.1016/j.ejmech.2020.112386

Reference: EJMECH 112386

To appear in: *European Journal of Medicinal Chemistry*

Received Date: 2 March 2020

Revised Date: 23 April 2020

Accepted Date: 23 April 2020

Please cite this article as: Z. Shi, N. Li, C. Chen, Y. Wang, Z. Lei, L. Chen, J. Sun, Novel NO-releasing scopoletin derivatives induce cell death via mitochondrial apoptosis pathway and cell cycle arrest, *European Journal of Medicinal Chemistry* (2020), doi: https://doi.org/10.1016/j.ejmech.2020.112386.

Novel NO-releasing scopoletin derivatives induce cell death via mitochondrial apoptosis pathway and cell cycle arrest

Zhixian Shi[1], Na Li[1], Cheng Chen, Yujin Wang, Zhichao Lei, Li Chen*, and Jianbo Sun**

State Key Laboratory of Natural Medicines, Department of Natural Medicinal Chemistry, School of Traditional Chinese Pharmacy, China Pharmaceutical University, 24 Tong Jia Xiang, Nanjing 210009, People's Republic of China

** Corresponding author: Tel: +86 83271447*

E-mail address: chenli627@cpu.edu.cn (Li Chen)

*** Corresponding author: Tel: +86 83271415*

sjbcpu@gmail.com (Jianbo Sun)

[1]These authors contributed equally.

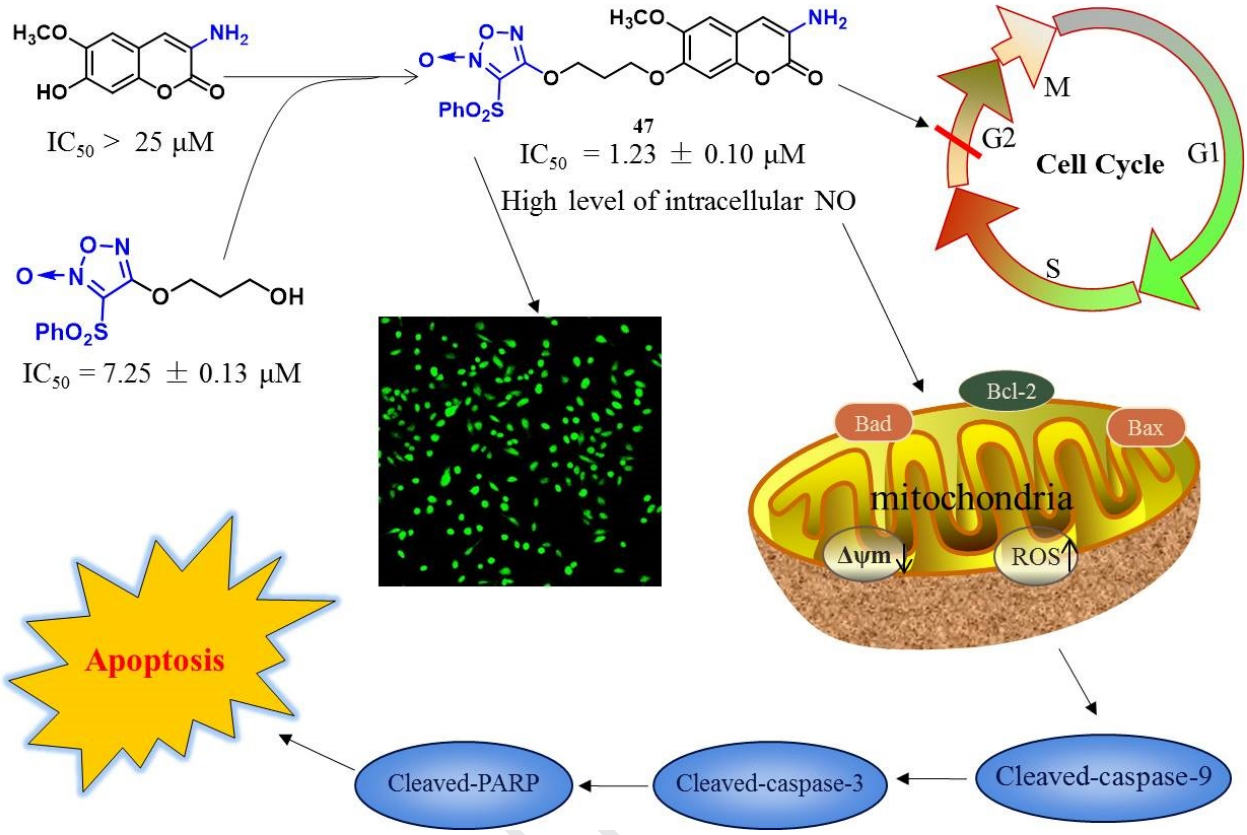

Novel NO-releasing scopoletin derivatives induce cell death via mitochondrial apoptosis pathway and cell cycle arrest

Zhixian Shi[1], Na Li[1], Cheng Chen, Yujin Wang, Zhichao Lei, Li Chen*, and Jianbo Sun**

State Key Laboratory of Natural Medicines, Department of Natural Medicinal Chemistry, School of Traditional Chinese Pharmacy, China Pharmaceutical University, 24 Tong Jia Xiang, Nanjing 210009, People's Republic of China

** Corresponding author: Tel: +86 83271447*

E-mail address: chenli627@cpu.edu.cn (Li Chen); sjbcpu@gmail.com (Jianbo Sun)

[1]These authors contributed equally.

Abstract

A series of phenylsulfonyfuroxan-based NO-releasing scopoletin derivatives were designed and synthesized in the study. All target compounds showed significantly improved antiproliferative activity against four cancer cell lines (MDA-MB-231, MCF-7, HepG2 and A459) and lower cytotoxicity toward normal liver LO2 cells. Derivative **47** concentration-dependently inhibited the colony formation of MDA-MB-231 cells. NO-releasing assessment indicated that the intracellular NO level was almost positively correlated with the antiproliferative ability. Compound **47**, which released the highest amounts of NO, showed the best potency (IC_{50} = 1.23 μM) against MDA-MB-231 cells. Mechanism research revealed for the first time that **47** blocked the proliferation of MDA-MB-231 cells by activating mitochondrial apoptosis pathway and arresting cell cycle at G2/M phase. Taken together, as a novel scopoletin derivative, **47** exhibited excellent inhibitory effects against malignant cancer cells and lower toxicity on normal cells. Thus, an in-depth evaluation of **47** to explore its complete therapeutic potential for cancer treatment is warranted.

Key words: Scopoletin; Nitric oxide; Mitochondrial apoptosis pathway; Cell cycle arrest.

1. Introduction

Scopoletin (7-hydroxy-6-methoxy-2H-chromen-2-one) (Fig. 1), existing in diverse medicinal plants (*Scopolia japonica* Maxim., *Atropa belladonna* Linn., *Saposhnikovia divaricata* (Turcz.) Schischk., etc.) [1], possesses multiple pharmacological activities, including antitumor [2], antioxidant [3], and anti-inflammatory [4-5]. Of these, the favorable potency of scopoletin against various tumor cells has attracted many researchers' attention [6-9]. Further mechanism investigation demonstrates that scopoletin inhibits the multiplication of prostate cancer cells via inducing cell apoptosis and cell cycle arrest [10]. Similar results have also been reported in cholangiocarcinoma cells and cervical cancer cells [11-12]. Although scopoletin has no obvious toxicity on the viability of normal cells, the moderate or low anticancer activity hampers its clinical application. Therefore, considerable scopoletin derivatives have been designed and synthesized to enhance its antitumor activity [13-15]. Accordingly, for the past few years, our research group has been committed to designing scopoletin derivatives, and demonstrated that several compounds (such as compounds **1**-**4**, Fig. 1) exhibited superior antitumor activity compared to scopoletin *in vitro* [16-18]. However, the antitumor ability of these derivatives has not yet achieved desired effect, so further improvement is needed.

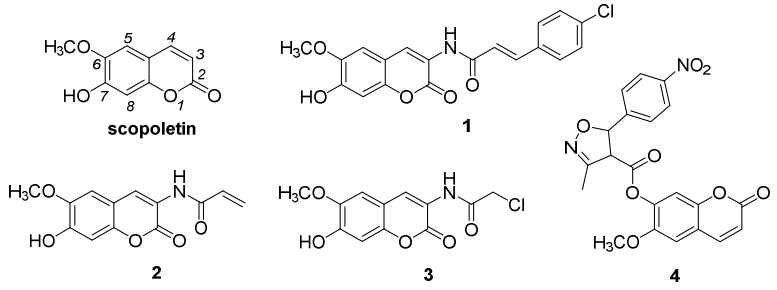

Fig. 1. Scopoletin and representative scopoletin derivatives

Hybridization strategy, chemically incorporating two or more pharmacophores with similar bioactivities to acquire a new molecular entity, has been widely and successfully applied in the discovery of anticancer drugs, antiviral drugs, etc. [19-21]. Nitric oxide (NO), an intracellular messenger molecule in cellular activities, has been proved to affect the progress of cancer cells *in vitro* and *in vivo* [22]. In cells, high levels of intracellular NO are involved in the up-regulation of signals such as p53, PARP, and DNA-PK, which can restrain DNA repair mechanisms [23]. Then, this process contributes to proliferation inhibition of cancer cells. Thus, many chemical NO donors have been developed to provide exogenous NO [24]. Among them, furoxan is an important NO donor and can generate high levels of intracellular NO. Particularly, as one of furoxan, phenylsulfonylfuroxan (Fig. 2) has been successfully applied for the design of anticancer hybrids [25-34]. For example, the furoxan-based NO-releasing hybrids **5-12** (Fig. 2) both exhibited improved antitumor activities *in vitro* compared with parent compounds. Hence, it is an effective way to enhance the antiproliferative activity of parent compounds by introducing phenylsulfonylfuroxan into their molecular structures while synthesizing NO-releasing hybrids.

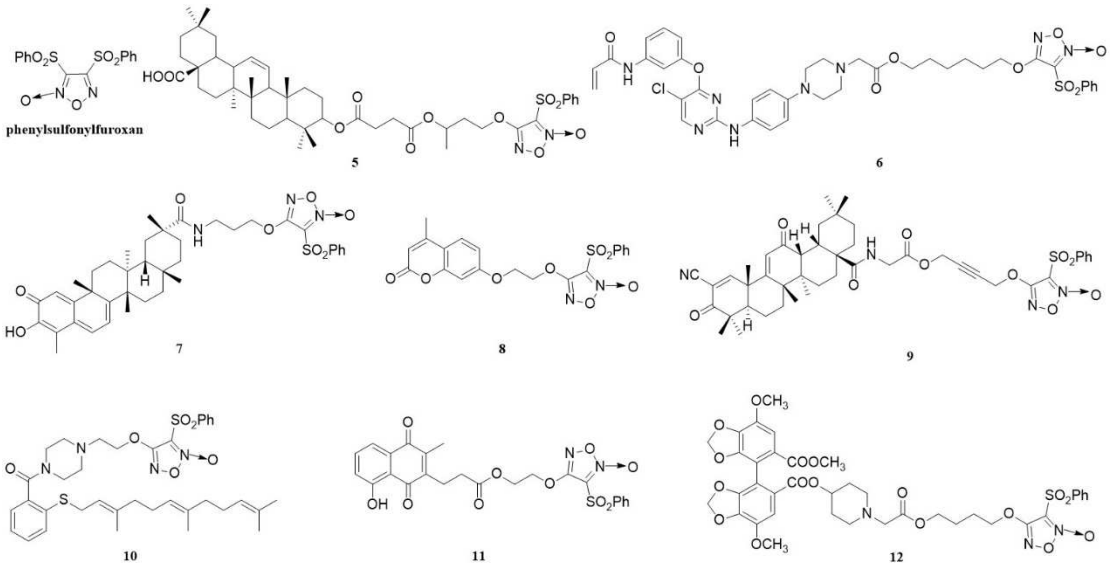

Fig. 2. Phenylsulfonylfuroxan and phenylsulfonylfuroxan-based hybrids

Thus, we attempted here to design novel NO-releasing scopoletin derivatives by introducing phenylsulfonylfuroxan at 7-position in scopoletin to enhance its antitumor effect (Fig. 3). In addition, given that introducing an acetylamino or amino group at 3-position of scopoletin is favorable for cytotoxic activity [14, 16-17], we also designed and synthesized a series of 3-acetylamino scopoletin/phenylsulfonylfuroxan and 3-amino scopoletin/phenylsulfonylfuroxan hybrids (Fig. 3). Their antiproliferative activities against cancer cells and cytotoxicities toward normal cells were measured. Further, the intracellular NO generated by target compounds was measured and the effect on antiproliferative activity was evaluated. Moreover, we elucidated the mitochondrial apoptotic pathway by apoptosis, mitochondrial membrane potential depolarization, ROS generation, and mitochondrial apoptosis protein determination. Simultaneously, cell cycle arrest was analyzed to explore further potential mechanism of these derivatives.

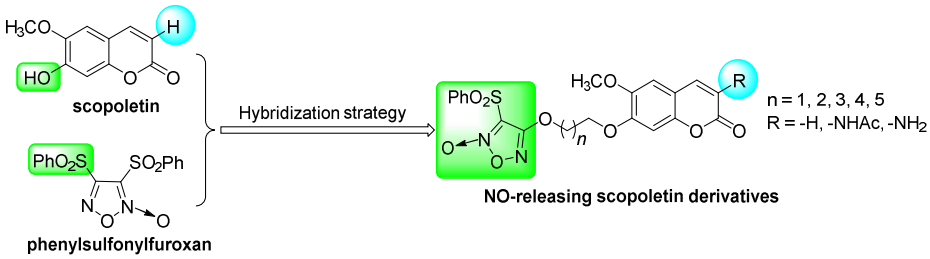

Fig. 3. The design of novel scopoletin/phenylsulfonyfuroxan hybrids

2. Results and discussion

2.1. Chemistry

The synthesis route of target compounds (**36-50**) is shown in Scheme 1. 3, 4-diphenylsulfonyl-furoxan (**15**) was obtained from benzenethiol (**12**) as described in the literature [35]. The starting material **12** was converted to 2-(phenylthio)acetic acid (**13**) via treatment with 2-chloroacetic acid, sodium hydroxide (NaOH), and sodium carbonate (Na_2CO_3). Following this, **13** was treated with hydrogen peroxide (H_2O_2) to generate (phenylsulfonyl)methanoic acid (**14**), which was then mixed with fuming nitric acid to provide intermediate **15**. Further, scopoletin and **20a** were synthesized from 2,4,5-trimethoxybenzaldehyde (**16**) according to the method reported by our group [16-18]. Compound **20b** was obtained from intermediate **19** in the presence of hydrochloric acid [36]. Subsequently, intermediate scopoletin, **20a**, and **20b** were separately treated with different halo alcohols to yield compounds **21**-**35**. Finally, **21**-**35** were treated separately with **15** to provide target compounds **36**-**50** in the presence of 8-diazabicyclo [5.4.0] undec-7-ene (**DBU**) [25].

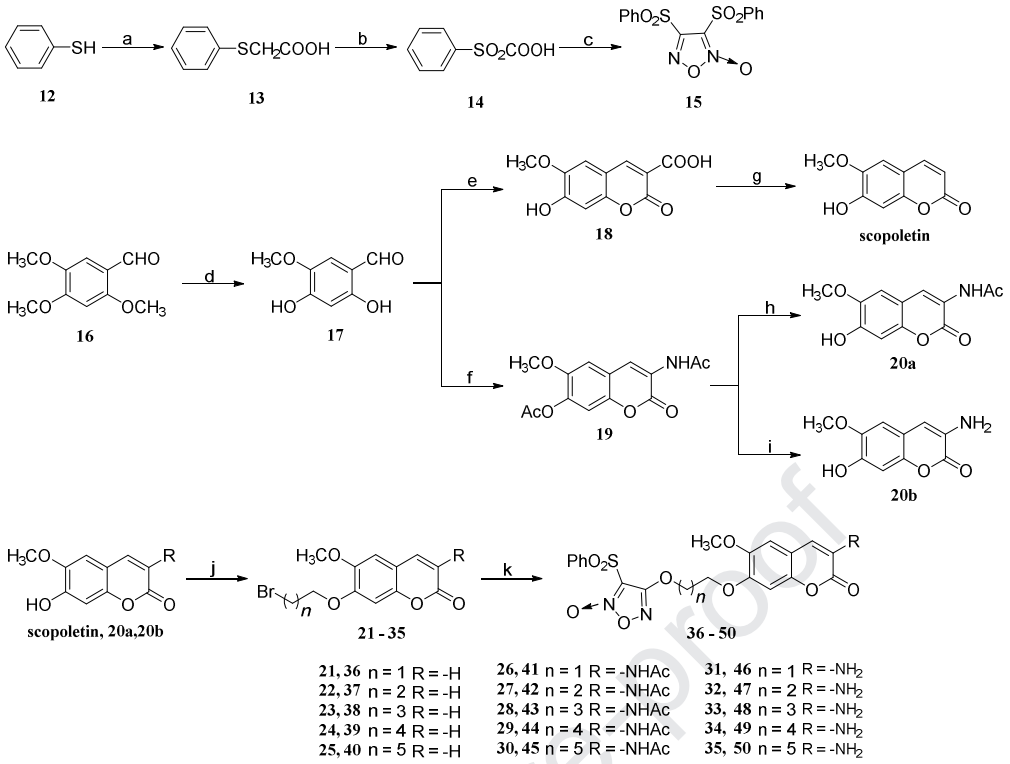

Scheme 1. Reagents and conditions: (a) $ClCH_2COOH$, Na_2CO_3, NaOH, EtOH, reflux, 4h; (b) H_2O_2, AcOH, rt, 3h; (c) fuming HNO_3, reflux, 4h; (d) $AlCl_3$, CTAB, dry DCM, reflux, 4h; (e) malonic acid, aniline, pyridine, rt, 24h; (f) glycine, Ac_2O, NaOAc, reflux, 4h; (g) pyridine, reflux, 6h; (h) K_2CO_3, MeOH, reflux, 1h; (i) EtOH, HCl, 80°C, 1h; (j) $BrCH_2(CH_2)_nOH$, DMF, 60°C, 8h; (k) **15**, DBU, DCM, -15°C, 4h;

2.2. Antiproliferative activity in vitro

Firstly, we measured the proliferation inhibition rates of scopoletin, **20a**, **20b**, and **36**-**50** in MCF-7 cells via the MTT assay at a concentration of 10 μM. All target compounds (**36**-**50**) showed favorable inhibitory effect on MCF-7 cell proliferation (inhibition rates: 48.63%-91.55%) (Table 1). However, the proliferation inhibition rates of **20a** and **20b** (7.95%, 5.21%, 7.13% respectively) were not significantly different, suggesting that the introduction of either acetylamino or amino at C-3 position without other modifications failed to boost up the antiproliferative activity.

Table 1. The proliferation inhibition rates of the tested compounds in MCF-7 cells

Cpd.	IR (%)[a]	Cpd.	IR (%)[a]
36	89.19	**45**	48.63
37	88.57	**46**	88.55
38	84.37	**47**	91.55
39	87.06	**48**	89.02
40	84.80	**49**	88.78
41	83.72	**50**	84.37
42	88.51	Scopoletin	7.95
43	80.41	**20a**	5.21
44	73.64	**20b**	7.13

[a] IR, inhibition rate, MCF-7 cells were treated with the tested compounds (10 μM) for 48 h (mean ± SD, n = 3)

Next, the target compounds **36-50** were tested in the following cancer cell lines: MDA-MB-231, MCF-7, HepG2, and A549. Doxorubicin was selected as positive control. As shown in Table 2, compared with scopoletin, **36-50** showed potential anticancer potency in all studied cancer cells. Further, compounds **36-50** showed higher activities in MDA-MB-231, MCF-7, and HepG2 than in A549, indicating the selectivity of these scopoletin derivatives against different tumor cells. Subsequently, **36-50** were also studied in human normal liver cell line LO-2 for evaluating their cytotoxicity towards normal cells. All scopoletin derivatives exhibited reduced cytotoxicity toward LO-2 cell (IC_{50} = 7.82-17.33 μM) compared with cancer cell lines.

Among all derivatives, compound **47** was the most active derivative with an IC_{50} of 1.23 μM in MDA-MB-231, slightly higher than that of doxorubicin (IC_{50} = 0.55 μM) (Table 2). However, compound **47** showed approximately 15-fold less toxic than doxorubicin in LO-2 cell (IC_{50} = 0.59 μM).

With an amino group in C-3 position, compound **50** did not show favorable antiproliferative activities in all cell lines except HepG2 due to six carbons in the linker. Similar results were also observed in derivatives **36**-**45**, which shared the same substituent group at C-3 position. Compounds **40** and **45** showed inferior antitumor effects also due to their six carbon length linkers. Although such scopoletin derivatives with acetamido or amino group attached (compounds **36-40** or **41-45** or **46-50**) have no significant difference in anticancer activity, scopoletin derivatives still show a certain pattern structure-activity relationship. According to biological studies conducted in 3-acetylamino scopoletin/phenylsulfonylfuroxan hybrids (compounds **41**-**45**), the introduction of acetamido is generally not conducive to anticancer efficacy, but compound **42** showed potential antitumor activity in MCF-7 and HepG2 cells. The activity difference between scopoletin/phenylsulfonylfuroxan and 3-amino scopoletin/phenylsulfonylfuroxan (compounds **36**-**39** and **46**-**49)** is the smallest; compounds **37** and **47** have the highest activity among all derivatives. Unfortunately, compound **37** was more active than **47** in LO-2. Overall, the biological data shown in Table 2 revealed that these modifications to scopoletin resulted in increased anticancer activity, and the most active compound (**47**) was selected for further study.

Table 2 The IC_{50} values of **36**-**50** against cancer cell lines and human liver LO2 cells

Compounds	IC_{50} (μM)[a]				
	MDA-MB-231	MCF-7	HepG2	A549	LO2
36	2.86 ± 0.11	3.54 ± 0.11	3.61 ± 0.16	7.24 ± 0.37	10.94 ± 0.52
37	1.85 ± 0.08	2.27 ± 0.12	2.90 ± 0.19	5.45 ± 0.14	7.82 ± 0.23
38	2.79 ± 0.14	3.04 ± 0.06	3.25 ± 0.15	6.14 ± 0.30	9.33 ± 0.16
39	3.17 ± 0.16	3.85 ± 0.13	3.42 ± 0.21	10.62 ± 0.09	8.86 ± 0.53
40	3.35 ± 0.06	4.48 ± 0.32	3.79 ± 0.17	9.43 ± 0.15	12.42 ± 0.22
41	4.99 ± 0.25	6.89 ± 0.33	4.83 ± 0.18	8.79 ± 0.17	10.25 ± 0.12
42	3.81 ± 0.20	2.40 ± 0.18	2.82 ± 0.03	9.81 ± 0.13	8.36 ± 0.28
43	3.15 ± 0.14	3.44 ± 0.13	3.29 ± 0.07	7.19 ± 0.28	9.19 ± 0.04
44	4.34 ± 0.27	6.27 ± 0.21	5.42 ± 0.11	11.36 ± 0.30	13.76 ± 0.16
45	7.89 ± 0.16	11.30 ± 0.07	6.59 ± 0.11	14.95 ± 0.24	17.33 ± 0.21
46	2.46 ± 0.18	2.77 ± 0.24	3.06 ± 0.09	5.91 ± 0.13	9.82 ± 0.34
47	1.23 ± 0.10	1.91 ± 0.14	2.81 ± 0.13	4.18 ± 0.15	9.16 ± 0.38
48	1.93 ± 0.09	2.28 ± 0.15	2.64 ± 0.12	5.03 ± 0.21	8.63 ± 0.42
49	2.40 ± 0.13	2.62 ± 0.08	3.46 ± 0.16	6.88 ± 0.27	12.25 ± 0.41
50	2.93 ± 0.14	3.14 ± 0.17	3.06 ± 0.11	8.06 ± 0.22	10.26 ± 0.24
Scopoletin	>25	>25	>25	>25	>25
Doxorubicin[b]	0.55 ± 0.01	0.60 ± 0.04	0.62 ± 0.15	0.96 ± 0.06	0.59 ± 0.09

[a] MTT assay, cells were treated with tested compounds for 48 h (mean ± SD, n = 3)
[b] Positive control

*2.3. Effect of compound **47** on colony formation*

Plate clone formation assay was performed to evaluate the effect of **47** on cellular proliferative ability based on the colony forming efficiency. As presented in Fig. 4, at 0.25 μM, compound **47** slightly suppressed colony formation in MDA-MB-231 cell. Compared with control, the cells treated with 0.5 or 1 μM **47** displayed much smaller and fewer colonies, particularly those exposed to the higher drug concentration. The

absorbance after staining with crystal violet tested at 590 nm also decreased in dose-dependent manner. These results confirmed that **47** suppressed colony formation at nanomolar concentrations, and demonstrated the antiproliferative activity of **47** against MDA-MB-231 cell.

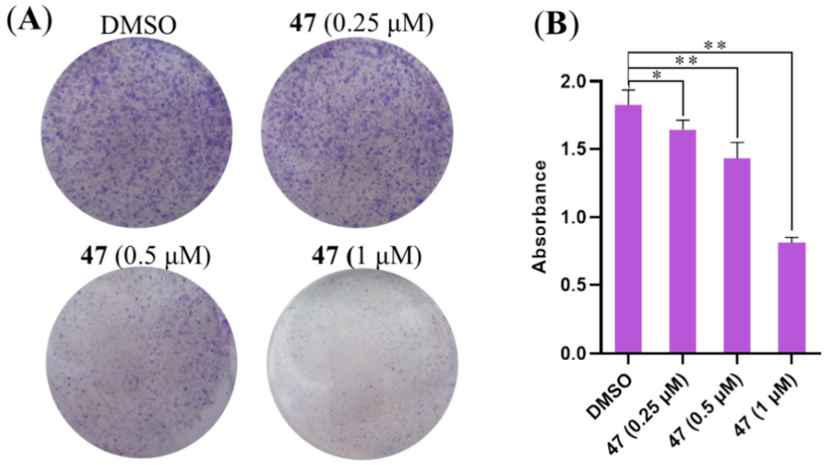

Fig. 4. Compound **47** inhibited the colony formation of MDA-MB-231 cells. (A) Cells were incubated with DMSO or **47** (0.25, 0.5, and 1 μM）for 24 h and then cultured in a fresh medium for another 10 days, followed by staining with crystal violet. (B) The absorbance of crystal after staining at 590 nm (mean ± SD, n = 3). **P < 0.01, *P < 0.05

2.4. Determination of intracellular NO

Cellular imaging, using the fluorescent probe DAF-FM DA, was conducted to determine whether **47** can release NO in MDA-MB-231 cells. As presented in Fig. 5A, after incubated with **47** (1 and 10 μM) for 2.5 h, the cells showed an increase of DAF-FM fluorescence intensity in a concentration-dependent manner. In contrast, no green fluorescence was observed in cells exposed to scopoletin. This result manifested that **47** can release NO in cells and implicated that all derivatives led to NO release in

MDA-MB-231cells.

Next, we used the total nitric oxide assay kit to quantify the levels of intracellular NO generated by all derivatives in MDA-MB-231 cell. As shown in Fig. 5B, intracellular NO levels after treatment with each synthesized hybrid for 2.5 h were different (approximately 3.99-10.33 μM). Treatment with compounds **46**-**50** resulted in higher levels of intracellular NO and showed higher anticancer potency among the target compounds. We speculate that the introduction of amino group increased the molecule polarity for improving lipo-hydro partition coefficient, which enable more drugs enter the cells and was beneficial to NO release. Derivative **47** with the highest anticancer potency showed the highest released levels of NO in MDA-MB-231 cell. The NO released by compound **37** was similar to that of **47**, indicating the potency of strong anticancer activities. Derivatives **36** and **38**-**45** showed moderate NO release, which indicated relatively poor potency. Therefore, the abilities of NO release for compounds **36**-**50** were generally positive consistent with their antitumor activities.

Furthermore, to investigate the relationship between NO release and antiproliferative activity of **47**, cells were pretreated with indicated concentrations of hemoglobin (NO scavenger). As presented in Fig. 5C, the proliferation inhibition rate decreased from 91.22% to 39.47% with an increasing concentration of hemoglobin (2.5-40 μM). The result indicated that the enhanced cytotoxicity of **47** towards MDA-MB-231 cell was partly due to the release of intracellular NO.

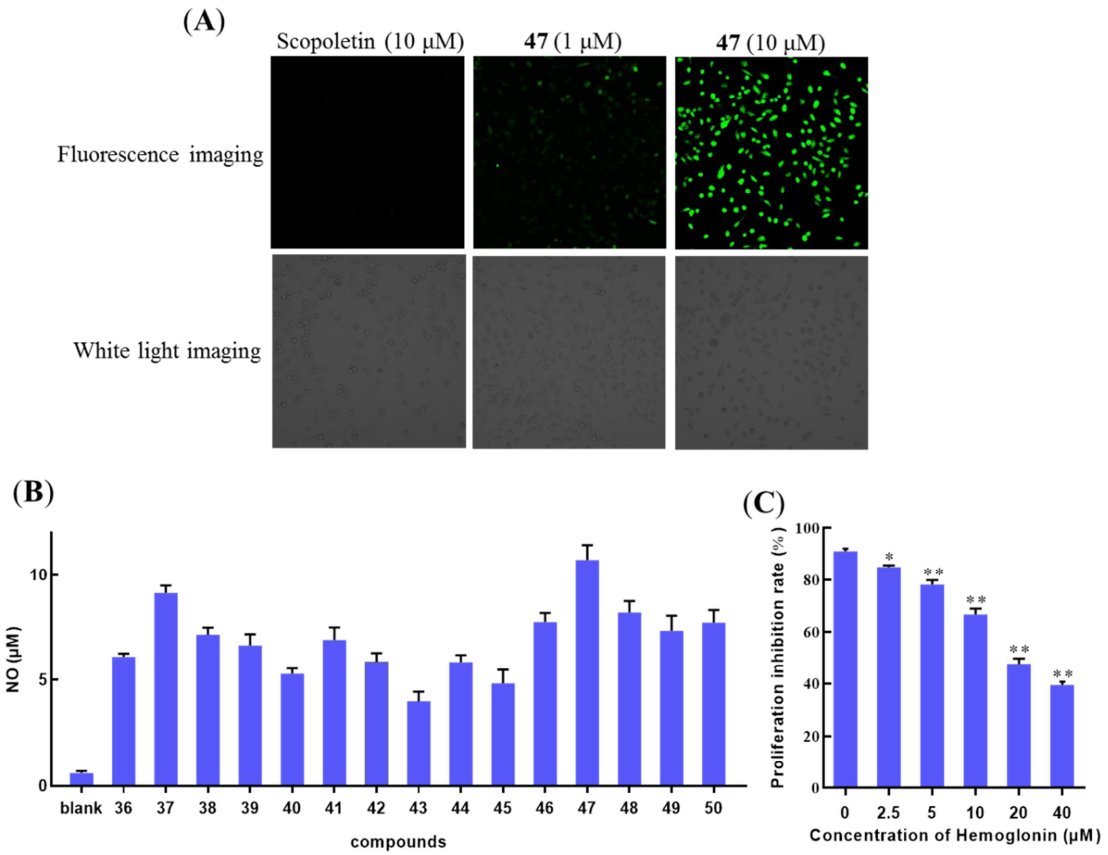

Fig. 5. Intracellular NO generated by the studied derivatives in MDA-MB-231 cells. (A) Cells were pretreated with DAF-FM DA and then incubated with scopoletin (10 μM) or **47** (1 and 10 μM) for 2.5 h, and then observed using a laser scanning confocal microscope (Olympus, Japan). (B) After cellular treatment with tested compounds (25 μM)) for 2.5 h, levels of intracellular NO were quantified using the total nitric oxide assay kit (mean ± SD, n = 3). (C) Cells were pretreated with hemoglobin (2.5, 5, 10, 20, and 40 μM) for 2 h and then incubated with **47** (4 μM) for another 48 h. The inhibition rates were measured by the MTT assay (mean ± SD, n = 3)

*2.5. Effect of an NO donor on the antiproliferative activity of **47***

To further explore the effect of NO on the antiproliferative activity, compound **47** was chemically split into two pharmacophores (compounds **51** and **52**), and their antiproliferative activities against MDA-MB-231 cell were measured by the MTT

assay (Fig. 6). The results showed that **47** (IC_{50} = 1.23 μM) was at least 5-fold and 8-fold more active than **51** (IC_{50} = 7.25 μM) and **52** (IC_{50} > 25 μM), respectively. Furthermore, **47** was significantly more active (by approximately 5-fold) when compared with the equimolar combination of **51** and **52** (1:1, IC_{50} = 6.36 μM), indicating the benefits of our derivative. These results indicated that the introduction of NO donor moieties was beneficial to anticancer potency, in line with the presumption of the NO-based hybrid design strategy.

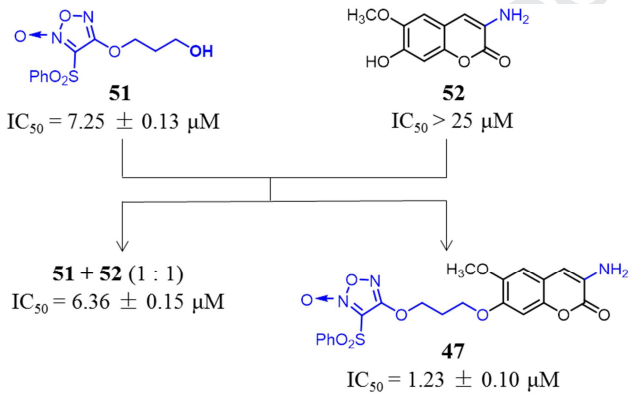

Fig. 6. Antiproliferative abilities of **51** and **52** and their equimolar mixture against MDA-MB-231 cells

*2.6. Compound **47** induced MDA-MB-231 cell death via apoptosis*

Apoptosis and necrocytosis are considered as two recognized pathways for anticancer agents due to their effects on cell survival and virulence [37]. To research the underlying mechanism of **47** on the proliferation inhibition of MDA-MB-231 cells, necrostatin-1 (necroptosis inhibitor) or Z-VAD-FMK (apoptosis inhibitor) was added prior to drug treatment. As presented in Fig. 7A, treatment with necrostatin-1 (10 μM) or Z-VAD-FMK (20 μM) showed no effect on cell viability in MDA-MB-231 cell. However, compared with cells treated with necrostatin-1, the inhibition rate of

MDA-MB-231 cell pretreated with Z-VAD-FMK decreased more significantly (Fig. 7B). The result suggested that derivative **47** induced the death of MDA-MB-231 cells via apoptosis pathway.

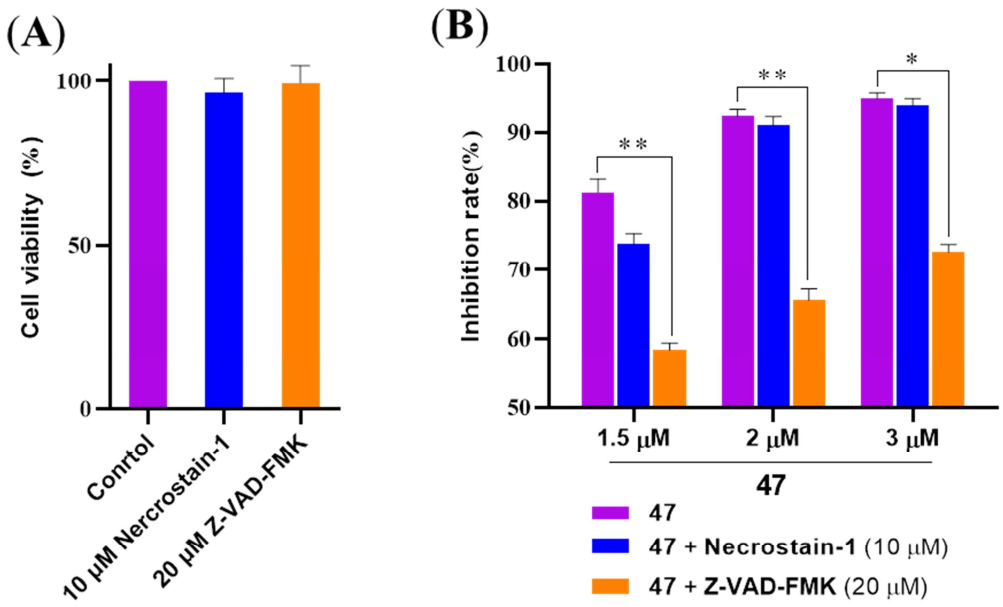

Fig. 7. (A) MDA-MB-231 cells were separately treated with necrostain-1 (10 μM) and Z-VAD-FMK (20 μM) for 48 h, and the cell viability was measured by MTT method. (B) Cells were pretreated with necrostatin-1 or Z-VAD-FMK for 1 h and then incubated with **47** (1.5, 2, and 3 μM) for another 48 h, and the inhibition rates were determined by MTT method (mean ± SD, n = 3). **P < 0.01, *P < 0.05

*2.7. Effect of **47** on cell apoptosis*

To confirm that compound **47** induced apoptosis of MDA-MB-231 cells, the Hoechst 33342 staining assay was performed (Fig. 8A). Compared with control cells, MDA-MB-231 treated with **47** for 24 h exhibited morphological apoptosis as judged from the bright blue stained apoptotic cells; the density of cells decreased dose-dependently, which was in agreement with the inhibitory effect of **47**. To further

confirm apoptosis induction by **47**, the cells were stained with Annexin V and PI and tested by flow cytometry. As observed in Fig. 8B and 8C, the proportion of total apoptotic (Q2 + Q3) cells increased from 9.9% to 34.0% in cells treated with compound **47** for 24 h; the early apoptotic cells (Q2) and late apoptotic cells (Q3) showed a similar increasing tendency. Based on these results, it was determined that compound **47** could induce the apoptosis of MDA-MB-231 cell.

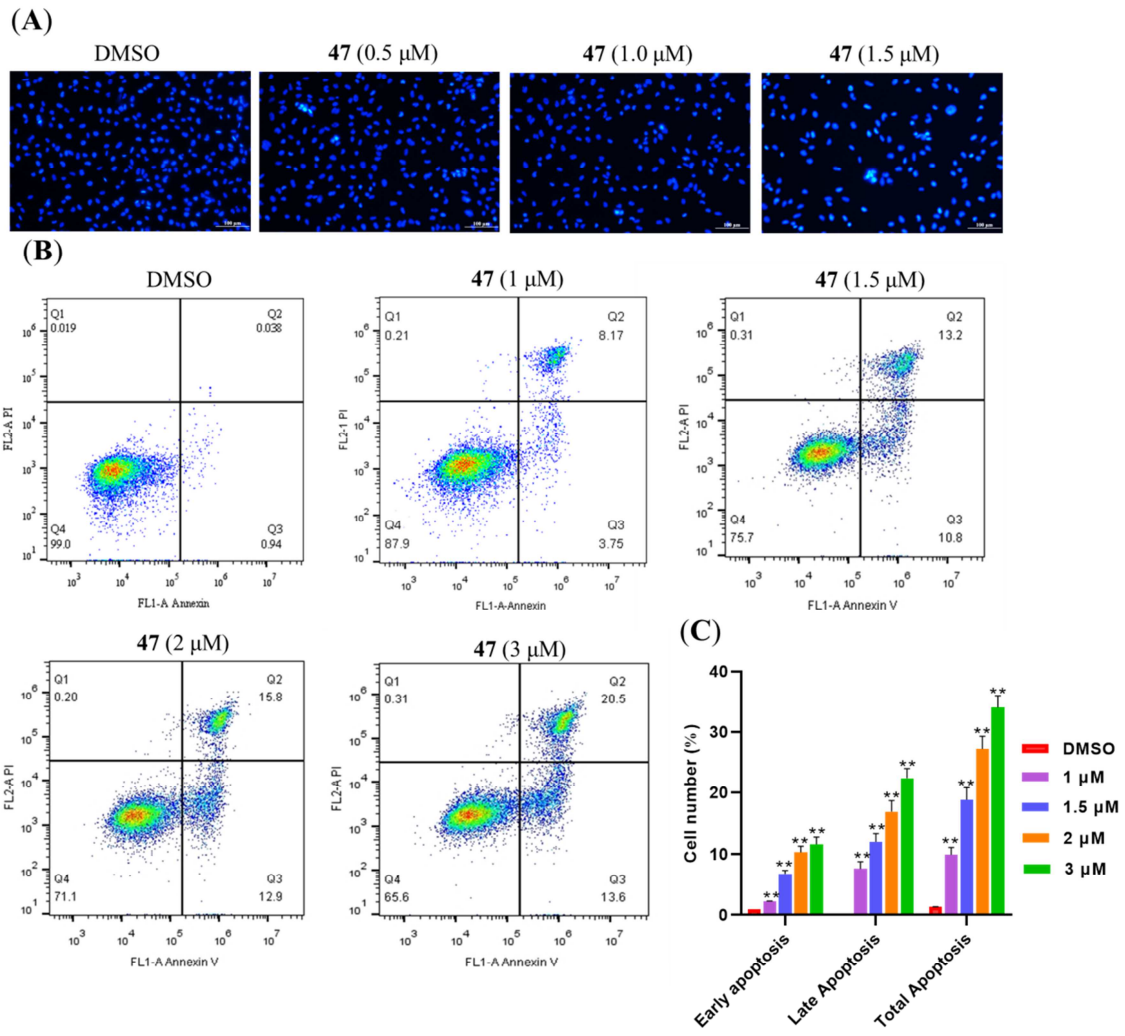

Fig. 8. Compound **47** induced the apoptosis of MDA-MB-231 cells. (A) Cells were treated with DMSO or **47** (0.5, 1, and 1.5 μM) for 24 h, and stained with Hoechst 33342. Cells were then observed under a fluorescent inverted microscope. (B) After

treatment with DMSO or **47** (1, 1.5, 2, and 3 μM) for 24 h, cells were collected and sequentially stained with Annexin V and Propidium Iodide (PI), followed by flow cytometric analysis. (C) The percentages of early, late, and total apoptotic cells were calculated (mean ± SD, n = 3). **P < 0.01, *P < 0.05 vs. the negative control group.

*2.8. Effect of **47** on the mitochondrial membrane potential*

Mitochondrial, death receptor, and endoplasmic reticulum stress-induced pathways are the three major apoptotic pathways [38]. The mitochondrion is a crucial cell organelle that regulates cellular survival and apoptosis, and many anticancer agents exhibit their pharmacological effects by acting on it. The mitochondrial function depends on the stabilization of the mitochondrial membrane structure [39], and scopoletin derivatives reported by our group can cause mitochondrial dysfunction [40]. Thus, we performed the JC-1 staining assay to estimate whether **47** had any effect on the mitochondrial membrane potential. Compared with the control group, the treatment group showed an increase in the proportion of cells with depolarized mitochondria (Q3) from 5.4% to 31.5% and a decrease in the proportion of hyperpolarized mitochondria (Q2) from 5.4% to 31.5% (Fig. 9). This result indicated that compound **47** induced the mitochondrial membrane potential depolarization in a concentration-dependent manner and disrupted mitochondrial function in MDA-MB-231 cells.

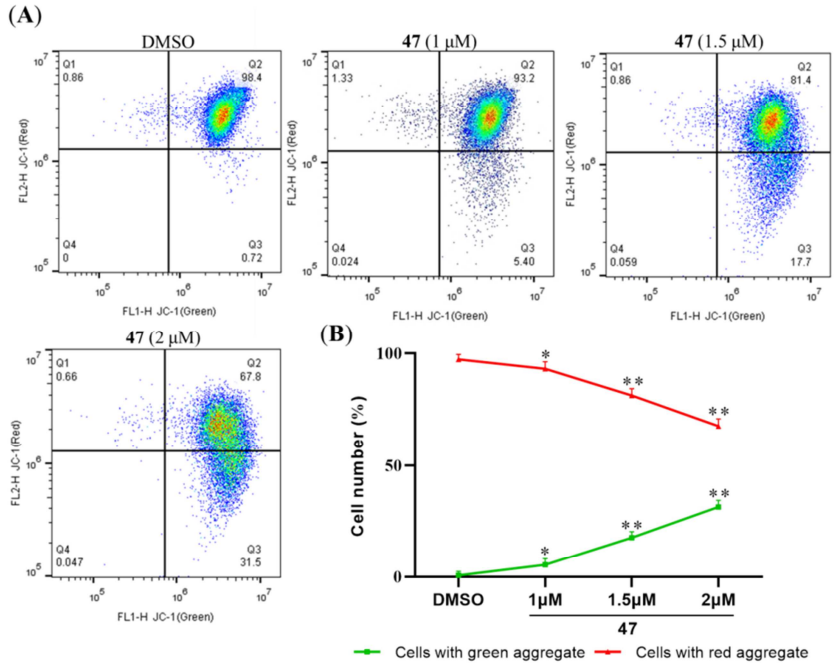

Fig. 9. Compound **47** affected the mitochondrial membrane potential of MDA-MB-231 cells. (A) Cells were treated with **47** (1, 1.5, and 2 μM) and DMSO (control) for 18 h, harvested, and then stained with JC-1, followed by flow cytometric analysis. (B) The percentage of cells with green fluorescence or red fluorescence was determined (mean ± SD, n = 3), **P < 0.01, *P < 0.05 vs. the negative control group.

*2.9. Effect of **47** on reactive oxygen species (ROS) generation*

Since the primary sources of ROS derived from mitochondria, the high level of intracellular ROS lead to the mitochondrial dysfunction and then activate apoptosis pathway [41]. To investigate whether **47** could promote the accumulation of ROS in MDA-MB-231 cell, the relative levels of ROS were monitored by DCF-DA staining assay and flow cytometric analysis. As presented in Fig. 10, the relative levels of ROS increased from 1.31 to 2.16 with the increase of the drug concentration, which showed significant difference compared with the levels observed in the control group. Pretreatment with NAC (N-acetyl-L-cysteine, ROS scavenger) before treatment with

47 (2 μM) resulted in a marked reduction in intracellular ROS levels; the relative levels of intracellular ROS decreased to 1.09, with no significant difference compared with control (Fig. 10). This result demonstrated that **47** was involved in ROS-induced apoptosis of MDA-MB-231 cell, which was associated with the mitochondrial apoptotic pathway.

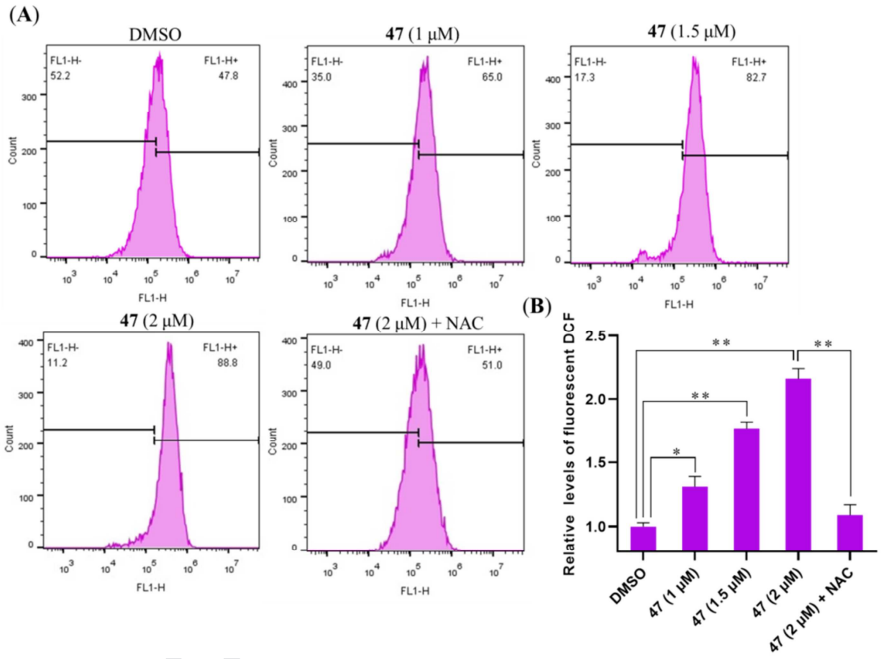

Fig. 10. Compound **47** induced ROS generation in MDA-MB-231 cells. (A) Cells were incubated with **47** (1, 1.5, and 2 μM) and DMSO (control) for 24 h, and then collected and stained with 2',7'-Dichlorofluorescin diacetate (DCFH-DA), followed by flow cytometric analysis. (D) The relative levels of fluorescent DCF were measured and plotted (mean ± SD, n = 3). **P < 0.01, *P < 0.05

*2.10. Compound **47** regulated the levels of mitochondrial apoptosis-related proteins*

The abovementioned experiments indicated that compound **47** induced cell death through the mitochondrial apoptotic pathway. The mitochondrial apoptotic pathway is mainly regulated by the Bcl family (e.g., Bcl-2, Bax, and Bad). Down-regulating the

level of Bcl-2 (an anti-apoptotic protein) and up-regulating the level of Bax and Bad (pro-apoptotic proteins) can increase the permeability of mitochondrial membrane [42]. Further, the increase in the permeability of the mitochondrial membrane promotes caspase-9 to form cleaved-caspase-9. Similarly, cleaved-caspase-3 is derived from caspase-3, which acts an executioner in the apoptotic signaling pathway. The cleaved-caspase-3 further cleaves PARP and eliminates PARP's ability to repair DNA, which is followed by apoptosis [42]. Therefore, we used western blot to thoroughly understand the effect of **47** on mitochondrial apoptosis-related proteins. Data from western blot showed that incubation of **47** reduced the expression of Bcl-2 in MDA-MB-231 cell, and the relative levels of Bax and Bad increased with the drug concentration (Fig. 11). This result indicated mitochondrial dysfunction, which was in accordance with **47**-induced mitochondrial depolarization concluded above. Bedsides, the relative levels of cleaved-caspase-3, cleaved-caspase-9, and cleaved-PARP increased in a concentration-dependent manner (Fig. 11). Taking into account the induced-apoptosis, mitochondrial depolarization, and ROS generation effects verified for our derivative, the mitochondrial apoptotic pathway was found to be responsible for the antiproliferative ability of **47**.

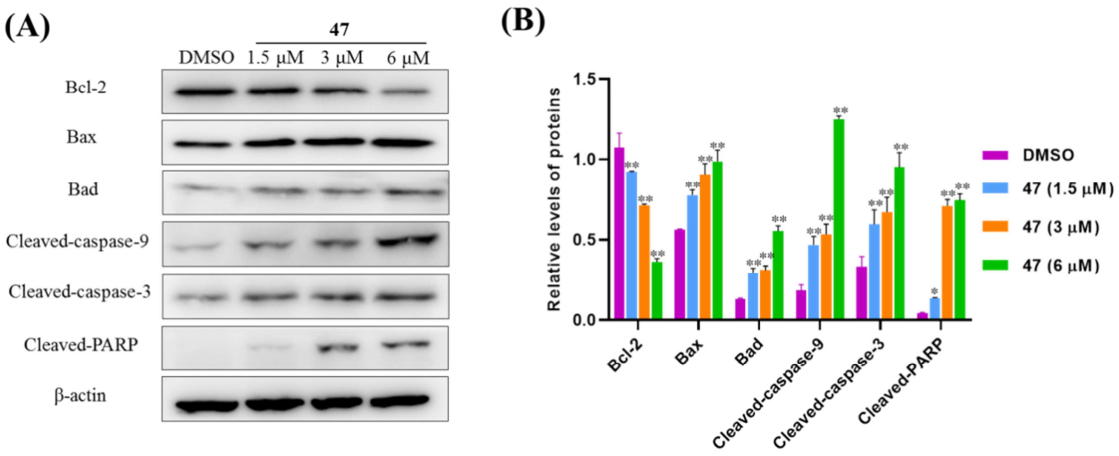

Fig. 11. Compound **47** affected the expressions of mitochondrial apoptosis-related proteins in MDA-MB-231 cells. (A) Cells were incubated with DMSO or **47** (1.5, 3, and 6 μM) for 8 h, and levels of Bcl-2, Bax, Bad, cleaved-caspase-9, cleaved-caspased-3, and cleaved-PARP were determined by western blotting. (B) Relative levels of mitochondrial apoptosis-related proteins were determined (mean ± SD, n = 3). **P < 0.01, *P < 0.05 vs. the negative control group

*2.11. Compound **47** blocked the Cell Cycle in the G2/M Phase*

Cell cycle is the basis of cell life activity and controls the entry of stationary phase cells into the proliferative phase [43]. Previous study showed that scopoletin could induce cell cycle at G2/M phase in HeLa cells [12]. To explore whether compound **47** had similar pharmacology function, PI staining assay and flow cytometry were performed. As shown in Fig. 12**,** compared with the control group, the treatment group showed a G2/M phase fraction of 24.58%, 30.11%, and 40.29% in MDA-MB-231 cells incubated with 1, 1.5, and 2 μM of **47**, respectively. However, the percentage of cells in G0/G1 and S phases decreased from 45.71% to 38.05% and 36.25% to 20.82%, respectively. This result proved that compound **47** could arrest cell cycle at G2/M phase in MDA-MB-231 cells, which was another important mechanism

for the antitumor effect of **47**.

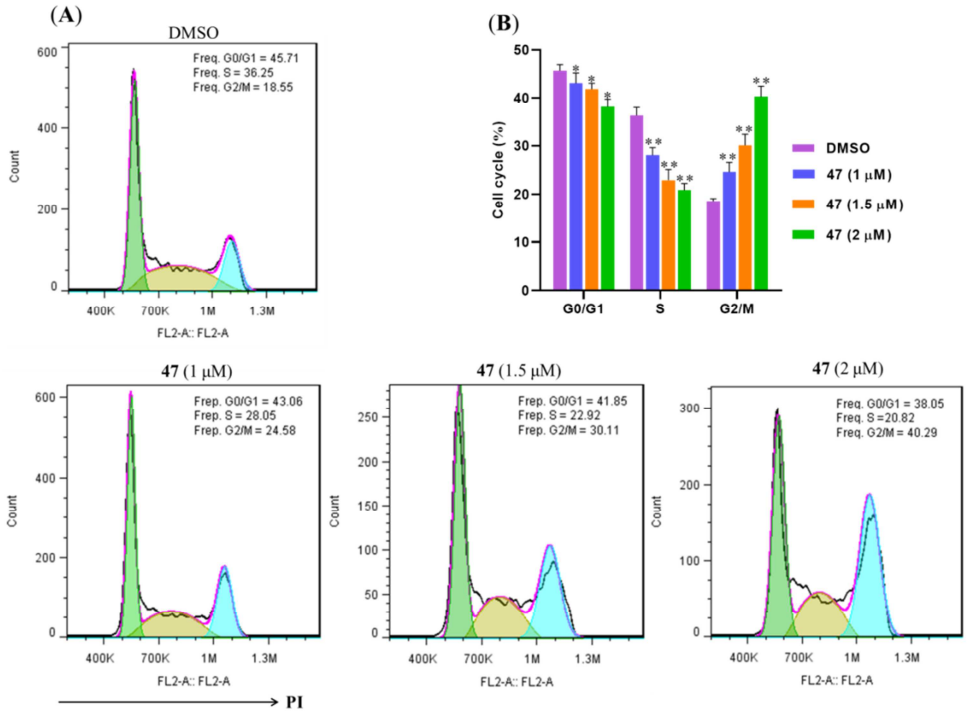

Fig. 12. Compound **47** blocked the cell cycle in the G2/M phase. (A) MDA-MB-231 cells were treated with **47** (1, 1.5, and 2 μM) or DMSO (control) for 24 h, and then collected, stained with PI, and analyzed by flow cytometric analysis. (B) The percentage of cells in each cell phase was determined (mean ± SD, n = 3). **P<0.01, *P<0.05 vs. the negative control group

3. Conclusions

A number of scopoletin derivatives were synthesized by introducing phenylsulfonyfuroxan moieties. All derivatives exhibited enhanced antiproliferative activities against cancer cell lines and reduced cytotoxicity toward normal cells. Derivative **47** was significantly more active than scopoletin and slightly weaker than doxorubicin against MDA-MB-231 cell. Analysis of NO release by our derivatives in MDA-MB-231 cell revealed that high anticancer potency of derivatives was

positively associated with their abilities to release intracellular NO. The mechanism research revealed that **47** induced mitochondrial depolarization and promoted intracellular ROS generation, and then regulated the expressions of mitochondrial apoptosis-related proteins (Bcl-2, Bax, Bad, Cleaved-caspase-3, Cleaved-caspase-9, Cleaved-PARP), finally activated the apoptosis. In addition, **47** arrested MDA-MB-231 cell cycle at the G2/M Phase. These derivatives blocked the growth of breast cancer MDA-MB-231 cell through mitochondrial apoptosis pathway and cell cycle arrest. Overall, compound **47** was a potential anticancer candidate and deserved further optimization.

4. Experimental protocol

4.1. Chemical Analysis

Reagents and solvents were commercially available. Each reaction was monitored by silica gel GF-254 plate at 254 nm or 365 nm ultraviolet light. Products were purified by recrystallization or silica gel column chromatography (200-300 mesh, Qingdao city, China). The structures of target compounds were confirmed by characterization with nuclear magnetic resonance (^{1}H NMR and ^{13}C NMR) and high resolution mass spectrometer (HRMS). NMR spectra were recorded on the Bruker AVANCE instrument (300 MHz) at 25°C using TMS as the internal standard in $CDCl_3$ or DMSO-d_6. HRMS was run on an Agilent Q-TOF mass spectrometer. The purity of scopoletin derivatives **36-50**, found in all cases as > 95%, was determined by SHIMADZU Prominence-i LC-2030C system equipped with a SHIMADZU Shim-pack GIST C18 4.6×250 mm (5 μm) column (column temperature equal 25ºC)

and a variable wavelength UVvis detector (detection at λ_{max} = 339 nm); the flow rates were 0.8 mL/min with injection volumes of 10 μL in acetonitrile mixtures and the mobile phase: 30:70 H_2O/CH_3CN. Intermediates **15**, scopoletin, **20a** and **20b** were obtained according to previous reported procedures [16-18, 33, 36].

*4.1.1. General procedure for synthesis of **36-50***

Respectively mixing intermediate scopoletin, **20a**, and **20b** (0.5 mmol) with indicated halo alcohol (0.6 mmol) in DMF (10 ml), K_2CO_3 (0.6 mmol) was added. The mixture was stirred at 60°C for 8 h. The mixture was cooled to room temperature, 10% NaOH aqueous solution was added into the mixture. Intermediate **21-35** were obtained by suction filtering, water washing, recrystallization with ethanol, and drying. Compounds **21-35** (0.3 mmol) separately reacted with **15** (0.45 mmol) in CH_2Cl_2 (10 ml) using **DBU** (1, 0.36 mmol) as a trigger. The mixture was stirred at -15°C for 4 h. Then, it was diluted with CH_2Cl_2 (20 ml), washed with 5% HCl, water, and dried over anhydrous Na_2SO_4, and then concentrated. The crude products were purified by silica gel column chromatography using CH_2Cl_2/MeOH (V/V, 150:1) to provide target compounds **36-50**.

4.1.1.1.

*4-(2-((6-methoxy-2-oxo-2H-chromen-7-yl)oxy)ethoxy)-3-(phenylsulfonyl)-1,2,5-oxadiazole 2-oxide (**36**).* White powder, 58.9% yield. Mp 203.8–205.4°C; ^{1}H NMR (300 MHz, DMSO-d_6) δ_H: 7.97–8.00 (2H, m), 8.00 (1H, d, *J* = 9.3 Hz), 7.77–7.82 (1H, m), 7.59–7.64 (2H, m), 7.29 (1H, s), 7.18 (1H, s), 6.36 (1H, d, *J* = 9.3 Hz), 4.83–4.85 (2H, m), 4.48–4.51 (2H, m), 3.79 (3H, s) ^{13}C NMR (75 MHz, DMSO-d_6) δ_C: 160.98,

159.42, 151.43, 149.64, 146.31, 144.72, 137.60, 136.44, 130.29 (C × 2), 128.64 (C × 2), 113.50, 112.18, 111.07, 109.78, 101.65, 70.14, 67.21, 56.38. HRMS (POSI) calculated for $C_{20}H_{17}N_2O_9S$ $[M+H]^+$ 461.06493, found 461.06527. Purity: 96.121% (by HPLC).

4.1.1.2.

*4-(3-((6-methoxy-2-oxo-2H-chromen-7-yl)oxy)propoxy)-3-(phenylsulfonyl)-1,2,5-oxadiazole 2-oxide (**37**).* White powder, 45.1% yield. Mp 196.8–198.4°C; ^{1}H NMR (300 MHz, DMSO-d_6) δ_H: 8.04 (1H, d, J = 9.6 Hz), 7.98–8.05 (2H, m), 7.84–7.90 (1H, m), 7.69–7.75 (2H, m), 7.29 (1H, s), 7.12 (1H, s), 6.35 (1H, d, J = 9.6 Hz), 4.60 (2H, t, J = 6.3 Hz), 4.23 (2H, t, J = 6.3 Hz), 3.81 (3H, s), 2.28–2.36 (2H, m). ^{13}C NMR (75MHz, DMSO-d_6) δ_C: 161.01, 159.29, 151.88, 149.75, 146.37, 144.76, 137.63, 136.51, 130.40 (C × 2), 128.81 (C × 2), 113.29, 111.87, 111.01, 109.60, 101.30, 68.70, 65.50, 56.38, 28.05. HRMS (POSI) calculated for $C_{21}H_{18}N_2NaO_9S$ $[M+Na]^+$ 497.06252, found 497.06244. Purity: 97.729% (by HPLC).

4.1.1.3

*4-(4-((6-methoxy-2-oxo-2H-chromen-7-yl)oxy)butoxy)-3-(phenylsulfonyl)-1,2,5-oxadiazole 2-oxide (**38**).* White powder, 25.9% yield. Mp 211.4–213.7°C; ^{1}H NMR (300 MHz, $CDCl_3$) δ_H: 8.01–8.04 (2H, m), 7.71–7.76 (1H, m), 7.61 (1H, d, J = 9.6 Hz), 7.56–7.61 (2H, m), 6.87 (1H, s), 6.86 (1H, s), 6.30 (1H, d, J = 9.6 Hz), 4.67 (2H, t, J = 6.0 Hz), 4.26 (2H, t, J = 6.0 Hz), 3.87 (3H, s), 2.41–2.49 (4H, m). ^{13}C NMR (75 MHz, DMSO-d_6) δ_C: 161.05, 159.32, 152.32, 149.86, 146.39, 144.80, 137.66, 136.57, 130.45 (C × 2), 128.77 (C × 2), 113.04, 111.58, 110.90, 109.45, 101.11, 71.82, 69.06,

56.33, 28.33, 28.00. HRMS (POSI) calculated for $C_{22}H_{20}N_2NaO_9S$ $[M+Na]^+$ 511.46603, found 511.46607. Purity: 98.326% (by HPLC).

4.1.1.4.

*4-((5-((6-methoxy-2-oxo-2H-chromen-7-yl)oxy)pentyl)oxy)-3-(phenylsulfonyl)-1,2,5-oxadiazole 2-oxide (**39**).* White powder, 37.1% yield. Mp 207.2–209.6°C; ^{1}H NMR (300 MHz, DMSO-d_6) δ_H: 8.03–8.06 (2H, m), 7.98 (1H, d, J = 9.6 Hz), 7.87–7.93 (1H, m), 7.73–7.78 (2H, m), 7.27 (1H, s), 7.12 (1H, s), 6.32 (1H, d, J = 9.6 Hz), 4.44 (2H, t, J = 6.3 Hz), 4.13 (2H, t, J = 6.3 Hz), 3.82 (3H, s), 1.80–1.91 (4H, m), 1.51–1.61(2H, m). ^{13}C NMR (75 MHz, DMSO-d_6) δ_C: 161.06, 159.34, 152.34, 149.88, 146.42, 144.81, 137.69, 136.58, 130.47 (C × 2), 128.78 (C × 2), 113.06, 111.60, 110.92, 109.49, 101.14, 71.84, 69.08, 56.36, 28.34, 28.02, 22.29. HRMS (POSI) calculated for $C_{23}H_{22}N_2NaO_9S$ $[M+Na]^+$ 525.09382, found 525.09375. Purity: 97.983% (by HPLC).

4.1.1.5.

*4-((6-((6-methoxy-2-oxo-2H-chromen-7-yl)oxy)hexyl)oxy)-3-(phenylsulfonyl)-1,2,5-oxadiazole 2-oxide (**40**).* White powder, 46.5% yield. Mp 201.9–203.6°C; ^{1}H NMR (300 MHz, DMSO-d_6) δ_H: 8.02–8.05 (2H, m), 7.97 (1H, d, J = 9.3 Hz), 7.89–7.93 (1H, m), 7.74–7.79 (2H, m), 7.27 (1H, s), 7.08 (1H, s), 6.31 (1H, d, J = 9.3 Hz), 4.42 (1H, t, J = 6.3 Hz), 4.11 (1H, t, J = 6.3 Hz), 3.83 (3H, s), 1.76–1.85 (4H, m), 1.40–1.55 (4H, m). ^{13}C NMR (75 MHz, DMSO-d_6) δ_C: 161.03, 159.32, 152.33, 149.85, 146.39, 144.77, 137.68, 136.56, 130.45 (C × 2), 128.75 (C × 2), 113.02, 111.55, 110.88, 109.48, 101.06, 71.83, 69.04, 56.36, 28.69, 28.20, 25.38, 25.12. HRMS (POSI)

calculated for $C_{24}H_{24}N_2NaO_9S$ $[M+Na]^+$ 539.10947, found 539.10953. Purity: 99.526% (by HPLC).

4.1.1.6.

*4-(2-((3-acetamido-6-methoxy-2-oxo-2H-chromen-7-yl)oxy)ethoxy)-3-(phenylsulfonyl)-1,2,5-oxadiazole 2-oxide (**41**).* White powder, 41.3% yield. Mp 205.4–207.0°C; ^{1}H NMR (300 MHz, DMSO-d_6) δ_H: 9.67 (1H, s), 8.63 (1H, s), 7.97–8.00 (2H, m), 7.78–7.83 (1H, m), 7.59–7.65 (2H, m), 7.33 (1H, s), 7.17 (1H, s), 4.84 (2H, s), 4.48 (2H, s), 3.78 (1H, s), 2.19 (3H, s). ^{13}C NMR (75 MHz, DMSO-d_6) δ_C: 170.43, 159.44, 158.32, 149.61, 146.84, 145.25, 137.60, 136.48, 130.31 (C × 2), 128.65 (C × 2), 125.33, 122.85, 112.77, 110.08, 109.57, 101.55, 70.23, 68.94, 56.43, 24.34. HRMS (POSI) calculated for $C_{22}H_{20}N_4O_{10}S$ $[M+NH_4]^+$ 535.11294, found 535.11298. Purity: 99.649% (by HPLC).

4.1.1.7.

*4-(3-((3-acetamido-6-methoxy-2-oxo-2H-chromen-7-yl)oxy)propoxy)-3-(phenylsulfonyl)-1,2,5-oxadiazole 2-oxide (**42**).* White powder, 46.7% yield. Mp 196.4–198.1°C; ^{1}H NMR (300 MHz, DMSO-d_6) δ_H: 9.66 (1H, s), 8.61 (1H, s), 8.01–8.04 (2H, m), 7.84–7.89 (1H, m), 7.69–7.74 (2H, m), 7.32 (1H, s), 7.11 (1H, s), 4.59 (2H, t, J = 6.0 Hz), 4.20 (2H, t, J = 6.0 Hz), 3.80 (3H, s), 2.29–2.32 (2H, m), 2.18 (3H, s). ^{13}C NMR (300MHz, DMSO-d_6) δ_C: 170.34, 159.33, 158.34, 150.51, 146.89, 145.46, 137.67, 136.57, 130.46 (C × 2), 128.75 (C × 2), 125.51, 122.49, 112.03, 110.88, 109.26, 100.88, 71.83, 68.96, 56.40, 28.75, 24.31. HRMS (POSI) calculated for $C_{23}H_{22}N_3O_{10}S$ $[M+H]^+$ 532.10204, found 532.10229. Purity: 98.898% (by HPLC).

4.1.1.8.

*4-(4-((3-acetamido-6-methoxy-2-oxo-2H-chromen-7-yl)oxy)butoxy)-3-(phenylsulfonyl)-1,2,5-oxadiazole 2-oxide (**43**).* White powder, 28.6% yield. Mp 198.0–199.3°C; ^{1}H NMR (300 MHz, DMSO-d_6) δ_H: 9.64 (1H, s), 8.60 (1H, s), 8.02–8.05 (2H, m), 7.88–7.93 (1H, m), 7.75–7.77 (2H, m), 7.31 (1H, s), 7.11 (1H, s), 4.52 (2H, t, *J* = 6.0 Hz), 4.16 (2H, t, *J* = 6.0 Hz), 3.81 (3H, s), 2.17 (3H, s), 1.86–2.01 (4H, m). ^{13}C NMR (75 MHz, DMSO-*d*6) δ_C: 170.34, 159.33, 158.34, 150.51, 146.89, 145.45, 137.67, 136.57, 130.46 (C × 2), 128.75 (C × 2), 125.51, 122.49, 112.03, 110.88, 109.25, 100.88, 71.83, 68.95, 56.40, 28.75, 28.20, 24.30. HRMS (POSI) calculated for $C_{24}H_{23}N_3NaO_{10}S$ $[M+Na]^+$ 568.09964, found 568.09998. Purity: 99.015% (by HPLC).

4.1.1.9.

*4-((5-((3-acetamido-6-methoxy-2-oxo-2H-chromen-7-yl)oxy)pentyl)oxy)-3-(phenylsulfonyl)-1,2,5-oxadiazole 2-oxide (**44**).* White powder, 35.4% yield. Mp 204.7–205.9°C; ^{1}H NMR (300 MHz, DMSO-d_6) δ_H: 9.73 (1H, s), 8.69 (1H, s), 8.12–8.15 (2H, m), 7.97–8.02 (1H, m), 7.82–7.87 (2H, m), 7.39 (1H, s), 7.20 (1H, s), 4.54 (2H, t, *J* = 6.0 Hz), 4.19 (2H, t, *J* = 6.0 Hz), 3.91 (3H, s), 2.27 (3H, s), 1.91–1.95 (4H, m), 1.62–1.69 (2H, m). ^{13}C NMR (75MHz, DMSO-d_6) δ_C: 170.34, 159.32, 158.36, 150.50, 146.89, 145.46, 137.66, 136.57, 130.46 (C × 2), 128.77 (C × 2), 125.53, 122.50, 112.06, 110.90, 109.25, 100.96, 71.83, 68.99, 56.38, 28.38, 28.01, 24.31, 22.29. HRMS (POSI) calculated for $C_{25}H_{25}N_3NaO_{10}S$ $[M+Na]^+$ 582.11529, found 582.11527. Purity: 99.578% (by HPLC).

4.1.1.10.

*4-((6-((3-acetamido-6-methoxy-2-oxo-2H-chromen-7-yl)oxy)hexyl)oxy)-3-(phenylsulf onyl)-1,2,5-oxadiazole 2-oxide (**45**).* White powder, 54.1% yield. Mp 192.1–194.3°C; ^{1}H NMR (300 MHz, DMSO-d_6) δ_H: 9.63 (1H, s), 8.60 (1H, s), 8.02–8.05 (2H, m), 7.89–7.94 (1H, m), 7.74–7.80 (1H, m), 7.30 (1H, s), 7.07 (1H, s), 4.42 (2H, t, J = 6.3 Hz), 4.08 (2H, t, J = 6.3 Hz), 3.83 (3H, s), 2.18 (3H, s), 1.78–1.82 (4H, m), 1.45–1.55 (4H, m). ^{13}C NMR (75 MHz, DMSO-d_6) δ_C: 170.32, 159.32, 158.34, 150.52, 146.90, 145.46, 137.68, 136.56, 130.45 (C × 2), 128.75 (C × 2), 125.50, 122.49, 112.03, 110.88, 109.27, 100.90, 71.84, 68.97, 56.41, 28.75, 28.21, 25.41, 25.14, 24.31. HRMS (POSI) calculated for $C_{26}H_{27}N_3NaO_{10}S$ $[M+Na]^+$ 596.13094, found 596.13049. Purity: 99.771% (by HPLC).

4.1.1.11.

*4-(2-((3-amino-6-methoxy-2-oxo-2H-chromen-7-yl)oxy)ethoxy)-3-(phenylsulfonyl)-1,2 ,5-oxadiazole 2-oxide (**46**).* Brown powder, 34.5% yield. Mp 183.6–185.7°C; ^{1}H NMR (300 MHz, DMSO-d_6) δ_H: 7.98–8.01 (2H, m), 7.79–7.84 (1H, m), 7.61–7.66 (2H, m), 7.08 (1H, s), 7.04 (1H, s), 6.75(1H, s), 4.79–4.81 (2H, m), 4.40–4.42 (2H, m), 3.76 (3H, s). ^{13}C NMR (75 MHz, DMSO-d_6) δ_C: 159.44 (C × 2), 146.79, 146.44, 142.87, 137.61, 136.46, 132.06, 130.31 (C × 2), 128.67 (C × 2), 115.27, 111.08, 109.44, 107.46, 102.14, 70.36, 67.18, 56.35. HRMS (POSI) calculated for $C_{20}H_{17}N_3NaO_9S$ $[M+Na]^+$ 498.05777, found 498.05770. Purity: 99.088% (by HPLC).

4.1.1.12.

*4-(3-((3-amino-6-methoxy-2-oxo-2H-chromen-7-yl)oxy)propoxy)-3-(phenylsulfonyl)-1 ,2,5-oxadiazole 2-oxide (**47**).* Brown powder, 28.1% yield. Mp 188.6–190.7°C; ^{1}H

NMR (300 MHz, DMSO-d_6) δ_H: 8.01–8.04 (2H, m), 7.84–7.89 (1H, m), 7.69–7.74 (2H, m), 7.03 (1H, s), 7.02 (1H, s), 6.75 (1H, s), 4.59 (2H, t, J = 6.0 Hz), 4.14 (2H, t, J = 6.0 Hz), 3.78 (3H, s), 2.24–2.32 (2H, m). ^{13}C NMR (75 MHz, DMSO-d_6) δ_C: 159.45, 159.30, 146.88, 146.80, 142.97, 137.64, 136.51, 131.90, 130.41 (C × 2), 128.80 (C × 2), 114.87, 110.99, 109.61, 107.31, 101.74, 68.77, 65.34, 56.33, 28.24. HRMS (POSI) calculated for $C_{21}H_{19}N_3NaO_9S$ $[M+Na]^+$ 512.07342, found 512.07329. Purity: 98.907% (by HPLC).

4.1.1.13.

*4-(4-((3-amino-6-methoxy-2-oxo-2H-chromen-7-yl)oxy)butoxy)-3-(phenylsulfonyl)-1,2,5-oxadiazole 2-oxide (**48**).* Brown powder, 13.7% yield. Mp 191.6–193.2°C; ^{1}H NMR (300 MHz, DMSO-d_6) δ_H: 8.02–8.05 (2H, m), 7.88–7.93 (1H, m), 7.72-7.78 (2H, m), 7.03 (2H, s), 6.74 (1H, s), 4.51 (2H, t, J = 6.3 Hz) , 4.09 (2H, t, J = 6.3 Hz), 3.79 (3H, S), 1.88–1.96 (4H, m). ^{13}C NMR (75 MHz, DMSO-d_6) δ_C: 159.46, 159.32, 147.18, 146.73, 143.05, 137.62, 136.58, 131.75, 130.45 (C × 2), 128.77 (C × 2), 114.52, 110.95, 109.73, 107.20, 101.43, 71.68, 68.50, 56.32, 28.52, 28.18. HRMS (POSI) calculated for $C_{22}H_{22}N_3O_9S$ $[M+H]^+$ 504.10713, found 504.10771. Purity: 98.493% (by HPLC).

4.1.1.14.

*4-((5-((3-amino-6-methoxy-2-oxo-2H-chromen-7-yl)oxy)pentyl)oxy)-3-(phenylsulfonyl)-1,2,5-oxadiazole 2-oxide (**49**).* Brown powder, 33.5% yield. Mp 197.1–199.4°C; ^{1}H NMR (300 MHz, DMSO-d_6) δ_H: 8.03–8.05 (2H, m), 7.87–7.92 (1H, m), 7.72–7.78 (2H, m), 7.02 (1H, s), 7.01 (1H, s), 6.75 (1H, s), 4.44 (2H, t, J = 6.3 Hz), 4.03 (2H, t,

J = 6.3 Hz), 3.79 (3H, S), 1.77–1.89 (4H, m), 1.54–1.57 (2H, m). ^{13}C NMR (75 MHz, DMSO-d_6) δ_C: 159.48, 159.32, 147.39, 146.77, 143.12, 137.68, 136.56, 131.63, 130.46 (C × 2), 128.77 (C × 2), 114.44, 110.90, 109.95, 107.25, 101.39, 71.86, 68.86, 56.32, 28.51, 28.03, 22.32. HRMS (POSI) calculated for $C_{23}H_{23}N_3NaO_9S$ $[M+Na]^+$ 540.10472, found 540.10562. Purity: 99.713% (by HPLC).

4.1.1.15.

*4-((6-((3-amino-6-methoxy-2-oxo-2H-chromen-7-yl)oxy)hexyl)oxy)-3-(phenylsulfonyl) -1,2,5-oxadiazole 2-oxide (**50**).* Brown powder, 47.3% yield. Mp 203.7–205.4°C, ^{1}H NMR (300 MHz, DMSO-d_6) δ_H: 8.02–8.05 (2H, m), 7.89–7.94 (1H, m), 7.74–7.79 (2H, m), 7.02 (1H, s), 6.99 (1H, s), 6.75 (1H, s), 4.42 (2H, t, *J* = 6.3 Hz), 4.02 (2H, t, *J* = 6.3 Hz), 3.80 (3H, s), 1.75–1.82 (4H, m), 1.38–1.54 (4H, m). ^{13}C NMR (75 MHz, DMSO-d_6) δ_C: 159.47, 159.33, 147.39, 146.77, 143.11, 137.69, 136.56, 131.62, 130.46 (C × 2), 128.75 (C × 2), 114.40, 110.88, 109.93, 107.27, 101.33, 71.85, 68.85, 56.34, 28.89, 28.22, 25.46, 25.17. HRMS (POSI) calculated for $C_{24}H_{25}N_3NaO_9S$ $[M+Na]^+$ 554.12037, found 554.12027. Purity: 99.707% (by HPLC).

4.2. Biological Experiments

Human cancer cells MDA-MB-231(human breast cancer cell line), MCF-7 (human breast cancer cell line) and HepG2 (human hepatocellular carcinoma cell line) were cultured in DMEM medium. A549 cells (human lung cancer cell line) were cultured in RPMI-1640 medium, as well as LO-2 cell line (human normal liver cell line). Each medium (KeyGEN, China) was supplemented with 10% fetal bovine serum (Gibco, USA). All the cell lines were obtained from National Infrastructure of Cell Line

Resource, China. Tested compounds were dissolved in DMSO (Sigma-Aldrich, USA) for usage, and the drug concentration was 10 mM.

4.2.1. Tested compounds' growth inhibition ratio in vitro.

MTT assay was used in this study for in vitro antitumor screening. The monolayer cell culture was trypsinized and the cell count was adjusted to 5×10^4 cells/ml. To each well of the 96 well microtiter plate, 0.1 mL of the diluted cell suspension (approximately 5,000 cells) was added. After 24 hours, when a partial monolayer was formed, the supernatant was replaced with 100 μL of fresh medium with different compound concentrations (0.5, 1, 2, 4, 10, and 20 μM). The content of DMSO did not exceed 0.1%, and this concentration was found to be nontoxic to the cell lines. The cells were exposed to compounds for 48 hours at 37°C in a humidified atmosphere (90% RH) containing 5% CO_2. After that, MTT solution (KeyGEN, China) was added to the wells at the final concentration of 0.5 mg/ml and the plates were incubated for 4 hours at 37°C. The supernatant of each well was replaced with 100 μL of DMSO. The absorbance was determined at 570 nm by the microplate reader (POLA Rstar Omega, Germany). Cell survival was measured as the percentage absorbance compared to the control (nontreated cells). IC_{50} values were calculated with GraphPad Prism 8.0 software (California, USA). Doxorubicin and scopoletin was used as the internal standards. All cytotoxicity experiments were performed three times.

4.2.2. Plate clone formation assay

MDA-MB-231 cell suspension was seeded into 6-well cell culture plate (1.5×10^3 cells/well) and cultured for 24 hours. Discarding supernatant, and cells were cultured

in 1 ml of fresh medium with DMSO (1 μM) or different concentrations of **47** (0.25, 0.5, and 1 μM). After 24 hours, supernatant was replaced with fresh medium on an average day and cultured for another 10 days. Cells were washed with PBS twice and exposed to 1ml of 4% paraformaldehyde fix solution (Beyotime, China) for 0.5 hours at 4°C. Then, the supernatant was washed out, and cells were stained with crystal violet (Beyotime, China). 1 ml of DMSO was added into each well, the absorbance was measured at 590nm by the microplate reader (POLA Rstar Omega, Germany). The experiment was performed three times.

4.2.3. Fluorescence images of intracellular NO

0.5ml of MDA-MB-231 cell suspension was seeded into 24-well cell culture plate (5×10^4 cells/well) and incubated for 24 hours. The supernatant was replaced with 5 μM of DAF-FM DA solution (Beyotime, China) and cultured for 30 min at 37°C in 5% CO_2 cell incubator. Then, cells were washed with PBS and cultured in 0.5 ml of fresh medium with scopoletin (10 μM) or **47** (1 or 10 μM) for another 2.5 h. Cells were monitored by laser confocal microscope (Olympus FV3000, Japan).

4.2.4. Intracellular NO determination

Intracellular NO generated by tested compounds was measured according to total nitric oxide assay kit (Beyotime, China). 2 ml of MDA-MB-231 cell suspension was seeded into 6-well cell culture plate (2×10^5 cells/well) and cultured for 24 hours. Discarding supernatant, and cells were cultured in 2 ml of fresh medium with DMSO (25 μM) or tested compounds **36–50** (25 μM) for another 2.5 hours. Cells were harvested and lysed with 150 μL of buffer (For nitric oxide assay, Beyotime, China)

for 1h on ice. The NO concentration of lysis was measured according total nitric oxide assay kit (Beyotime, China). The experiment was performed three times.

4.2.5. Hoechst 33342 fluorescent staining

Hoechst 33342 (Beyotime, China) staining assay was used to explore the effect of **47** on morphological apoptosis. 0.5 ml of MDA-MB-231 cell suspension was seeded into 24-well cell culture plate (5×10^4 cells/well) and incubated for 24 hours. Discarding supernatant, and cells were cultured in 0.5 ml of fresh medium with DMSO (1.5 μM) or different concentration of **47** (0.5, 1, and 1.5 μM). After 24 hours, supernatant was replaced with 0.5 ml of Hoechst 33342 solution (10 μg/ml) and the plates were incubated for 5 min at 37°C in the dark. Washing with PBS twice and adding 0.5 ml of medium into each well. Cells were monitored by inverted fluorescence microscope (Nikon Ts2R, Japan).

4.2.6. Cell apoptosis analysis

Annexin V/PI apoptosis detection Kit (KeyGEN, China) was used to investigate the effect of **47** on apoptosis. 1 ml of MDA-MB-231 cell suspension was seeded into 6-well cell culture plate (2×10^5 cells/well) and cultured for 24 hours. Discarding supernatant, and cells were cultured in 1 ml of fresh medium with DMSO (3 μM) or different concentration of **47** (1, 1.5, 2, and 3 μM) for another 24 hours. Cells were collected and washed with PBS twice (2000 rpm, 5 min). Cells were suspended in 500 μL binding buffer, and Annexin (5 μL) and PI (5 μL) were added respectively. Then, cells were incubated for 30 min at 37 °C in the dark, followed by flow cytometer analysis (BD Accuri C6, American) . The experiment was performed three times.

4.2.7. Mitochondrial membrane potential analysis

The effect of **47** on mitochondrial membrane potential was evaluated by JC-1 apoptosis detection kit (KeyGEN, China). 1 ml of MDA-MB-231 cell suspension was seeded into 6-well cell culture plate (2×10^5 cells/well) and cultured for 24 hours. Discarding supernatant, and cells were cultured in 1 ml of fresh medium with DMSO (2 μM) or different concentration of **47** (1, 1.5, and 2 μM) for another 18 hours. Cells were collected and washed with PBS twice (2000 rpm, 5 min). Cells were incubated with JC-1 solution for 30 min at 37°C in the dark. Cells were washed with incubation buffer twice (2000 rpm, 5 min), and then suspended in incubation buffer, followed by flow cytometer analysis (BD Accuri C6, American). The experiment was performed three times.

4.2.8. Intracellular ROS analysis

Reactive oxygen species assay kit (Beyotime, China) was used to determine the intracellular ROS. 1 ml of MDA-MB-231 cell suspension was seeded into 6-well culture plate (2×10^5 cells/well) and cultured for 24 hours. Discarding supernatant, and cells were cultured in 1 ml of fresh medium with DMSO (2 μM) or different concentration of **47** (1, 1.5, and 2 μM) for another 24 hours. Cells were collected and incubated with DCFH-DA solution for 30 min at 37°C in the dark. Then, cells were collected and washed with PBS twice (2000 rpm, 5 min). Cells were suspended in medium without fetal bovine serum and analyzed by flow cytometer (BD Accuri C6, American). Cells were pretreated with 2.5 mM of NAC (N-acetyl-L-cysteine, Beyotime, China) for 2 h prior to incubation with 2 μM of **47**, and intracellular ROS

was tested by referring to the above method. The experiment was performed three times.

4.2.9. Western blot analysis

2 ml of MDA-MB-231 cell suspension was seeded into cell culture dish (60×15 mm) (8×10^5 cells/well) and cultured for 24 hours. Discarding supernatant, and cells were cultured in 2.0 ml of fresh medium with DMSO (6 μM) or different concentration of **47** (1.5, 3, and 6 μM) for another 8 hours. Cells were collected and lysed with lysis buffer (Beyotime, China). Proteins were diluted to 3 mg/ml according to BCA protein assay kit (Beyotime, China). Total proteins (30 μg) were separated by the SDS-PAGE (4~20% gel, Beyotime, China), transferred to PVDF membranes (0.45 μm, Beyotime, China), followed by blocking with QuickBlock™ blocking buffer (Beyotime, China). PVDF membranes were incubated with different primary antibodies respectively and followed by secondary antibodies. BeyoECL star assay kit (Beyotime, China) was used to visualize proteins bands. Proteins bands were analyzed by Image J software (NIH, Bethesda, MD, USA). All the primary antibodies (Anti-Bcl-2, Anti-Bax, Anti-Bad, Anti-Cleaved-caspase-9, Anti-Cleaved-caspase-3, Anti-PARP) were from Abcam, China, and secondary antibodies [HRP-labeled goat anti-rabbit IgG(H+L), HRP-labeled goat anti-mouse IgG(H+L)] were from Beyotime, China. The experiment was performed three times.

4.2.10. Cell cycle analysis

Cell cycle analysis kit (Beyotime, China) was used to explore the effect of **47** on cell cycle. 1 ml of MDA-MB-231 cell suspension was seeded into 6-well culture plate

(2×10^5 cells/well) and cultured for 24 hours. Discarding supernatant, and cells were cultured in 1 ml of fresh medium with DMSO (2 μM) or different concentration of **47** (1, 1.5, and 2 μM) for another 24 hours. Cells were collected and washed with PBS (2000 rpm, 5 min), and then were fixed with 70% ethanol at 4°C overnight. Cells were suspended in PBS (500 μL), and then stained with PI, followed by flow cytometer analysis (BD Accuri C6, American). The experiment was performed three times.

Associated content

Supporting Information

The supporting information is available free of charge on the Elsevier publications website at DOI: XXX.

Structural characterization of the target compounds **36–50** (^{1}H NMR, ^{13}C NMR, POSI/HRMS spectrum), and the HPLC analysis of **36–50**.

Author Information

Author Addresses: Tel: +86 83271415; *E-mail address: sjbcpu@gmail.com (Jianbo Sun); chenli627@cpu.edu.cn (Li Chen)*

Notes

The authors declare no competing financial interest.

Acknowledgements

This research has been supported by "Double First Class" Subject Innovation Team Construction Project of China Pharmaceutical University (CPU2018GY12), Natural

Science Foundation of Jiangsu Province, Grant/Award Number (BK20171394)，Key Laboratory for Tumour Precision Medicine of Shanxi Province Research Fund (KLTPM-SX2017-B1).

References

[1] G.J.B. Gnonlonfin, A. Sanni, L. Brimer, Review scopoletin - a coumarin phytoalexin with medicinal properties, Crit. Rev. Plant Sci. 31 (2012) 47-56.

[2] E.J. Seo, M. Saeed, B.Y.K. Law, A.G. Wu, O. Kadioglu, H.J. Greten, T. Efferth, Pharmacogenomics of scopoletin in tumor cells, Molecules. 21 (2016) 496.

[3] A. Witaicenis, L.N. Seito, A.D. Chagas, L.D. de Almeida Junior, A.C. Luchini, P. Rodrigues-Orsi, S.H. Cestari, L.C. Di Stasi, Antioxidant and intestinal anti-inflammatory effects of plant-derived coumarin derivatives, Phytomedicine. 21 (2014) 240-246.

[4] H.J. Kim, S.I. Jang, Y.J. Kim, H.T. Chung, Y.G. Yun, T.H. Kang, O.S. Jeong, Y.C. Kim, Scopoletin suppresses pro-inflammatory cytokines and PGE(2) from LPS-stimulated cell line, RAW 264.7 cells, Fitoterapia. 75 (2004): 261-266.

[5] P.D. Moon, B.H. Lee, H.J. Jeong, H.J. An, S.J. Park, H.R. Kim, S.G. Ko, J.Y. Um, S.H. Hong, H.M. Kim, Use of scopoletin to inhibit the production of inflammatory cytokines through inhibition of the I kappa B/NF-kappa B signal cascade in the human mast cell line HMC-1, Eur. J. Pharmacol. 555 (2007) 218-225.

[6] X.L. Liu, L. Zhang, X.L. Fu, K. Chen, B.C. Qian, Effect of scopoletin on PC3 cell proliferation and apoptosis, Acta Parmacol. Sin. 22 (2001) 929-933.

[7] M. Williams, J.M. Cassady, Potential antitumour agents: a cytotoxic cardenolides from oronilla varia L, J. Pharmacol. Sci. 65 (1976) 912-914.

[8] J.M. Cassady, N. Ojima, C. Chang, J. L. McLaughlin, An investigation of the antitumor activity of micromelum integerrimun (Rutaceae), J. Nat. Prod. 42 (1979) 274-278.

[9] M. Adams, T. Efferth, R. Bauer, Activity-guided isolation of scopoletin and isoscopoletin, the inhibitory active principles towards CCRF-CEM leukaemia cells and multi-drug resistant CEM/ADR5000 cells, from Artemisia argyi, Planta Med. 72 (2006) 862-864.

[10] C.L. Li, X.C. Han, H. Zhang, J.S. Wu, B. Li, Effect of scopoletin on apoptosis and cell cycle arrest in human prostate cancer cells in vitro, Trop. J. Pharm. Res. 14 (2015) 611-617.

[11] M.A. Asgar, G. Senawong, B. Sripa, T. Senawong, Scopoletin potentiates the anticancer effects of cisplatin against cholangiocarcinoma cell lines, Bangl. J. Pharmacol. 10 (2015) 69-77.

[12] Q. Tian, L.Y. Wang, X. Sun, F. Zeng, Q. Pan, M. Xue, Scopoletin exerts anticancer effects on human cervical cancer cell lines by triggering apoptosis, cell cycle arrest, inhibition of cell invasion and PI3K/AKT signalling pathway, J. Buon. 24 (2019) 997-1002.

[13] H. Zou, H. Jiang, J.Y. Zhou, Y. Zhu, L. Cao, P. Xia, Q. Zhang, Synthesis of 3-(4-hydroxyphenyl)-4-methyl-6-methoxy-7-hydroxy-coumarinand its analogues as angiogenesis inhibitors, J. Chin. Pharm. Sci. 19 (2010) 136-140.

[14] W.K. Liu, J. Hua, J.P. Zhou, H.B. Zhang, H.Y. Zhu, Y.H. Cheng, R. Gust, Synthesis and in vitro antitumor activity of novel scopoletin derivatives, Bioorg. Med. Chem. Lett. 22 (2012) 5008-5012.

[15] X.T. Cai, J. Yang, J.P. Zhou, W.G Lu, C.P. Hu, Z.H. Gu, J.G. Huo, X.N. Wang, P. Cao, Synthesis and biological evaluation of scopoletin derivatives, Bioorg. Med. Chem. 21 (2013) 84-92.

[16] L.H. Li, P. Zhao, J.L. Hu, J.H. Liu, Y. Liu, Z.Q. Wang, Y.F. Xia, Y. Dai, L. Chen, Synthesis, in vitro and in vivo antitumor activity of scopoletin cinnamic acid hybrids, Eur. J. Med. Chem. 93 (2015) 30-107.

[17] W. Shi, J.L. Hu, N. Bao, D.G. Li, L. Chen, J.B. Sun, Design, synthesis and cytotoxic activities of scopoletin-isoxazole and scopoletin-pyrazole hybrids, Bioorg. Med. Chem. Lett. 27 (2017) 147-151.

[18] W. Shi, J.L. Zhang, N. Bao, F.Q. Guan, L. Chen, J.B. Sun, Design, synthesis, and cytotoxic evaluation of novel scopoletin derivatives, Chem. Biol. Drug Des. 91 (2017) 1-6.

[19] Y. Tanaka, K. Aikawa, G. Nishida, M. Homma, S. Sogabe, S. Igaki, Y. Hayano, T. Sameshima, I. Miyahisa, T. Kawamoto, M. Tawada, Y. Imai, M. Inazuka, N. Cho, Y. Imaeda, T. Ishikawa, Discovery of potent Mcl-1/Bcl-xL dual inhibitors by using a hybridization strategy based on structural analysis of target proteins, J. Med. Chem. 56 (2013) 9635-9645.

[20] D.Y. Li, P. Zhan, E. De Clercq, X.Y. Liu, Strategies for the design of HIV-1 non-nucleoside reverse transcriptase inhibitors: lessons from the development of

seven representative paradigms, J. Med. Chem. 55 (2012) 3595-3613.

[21] R. Farina, L. Pisani, M. Catto, O. Nicolotti, D. Gadaleta, N. Denora, R. Soto-Otero, E. Mendez-Alvarez, C.S. Passos, G. Muncipinto, C.D. Altomare, A. Nurisso, P.A. Carrupt, A. Carotti, Structure-based design and optimization of multitarget-directed 2H-Chromen-2-one derivatives as potent inhibitors of monoamine oxidase B and cholinesterases, J. Med. Chem. 58 (2015) 5561-5578.

[22] P. Pacher, J.S. Beckman, L. Liaudet, Nitric oxide and peroxynitrite in health and disease, Physiol. Rev. 87 (2007) 315-424.

[23] W.M. Xu, L.Z. Liu, M. Loizidou, M. Ahmed, I.G. Charles, The role of nitric oxide in cancer, Cell Res. 12 (2002) 311-320.

[24] A.A. Eroy-Reveles, Y. Leung, C.M. Beavers, M.M. Olmstead, P.K. Mascharak, Near-infrared light activated release of nitric oxide from designed photoactive manganese nitrosyls: Strategy, design, and potential as NO donors, J. Am. Chem. Soc. 130 (2008) 4447-4458.

[25] L. Chen, Y.H. Zhang, X.W. Kong, E. Lan, Z.J. Huang, S.X. Peng, D.L. Kaufman, J.D. Tian, Design, synthesis, and antihepatocellular carcinoma activity of nitric oxide releasing derivatives of oleanolic acid, J. Med. Chem. 51 (2008) 4834-4838.

[26] Y. Ling, X.L. Ye, Z.Z. Zhang, Y.H. Zhang, Y.S. Lai, H. Ji, S.X. Peng, J.D. Tian, Novel Nitric Oxide-Releasing Derivatives of Farnesylthiosalicylic Acid: Synthesis and Evaluation of Antihepatocellular Carcinoma Activity, J. Med. Chem. 54 (2011) 3251-3259.

[27] C. Han, Z.J. Huang, C. Zheng, L.D. Wan, L.W. Zhang, S.X. Peng, K. Ding, H.B. Ji, J.D. Tian, Y.H. Zhang, Novel Hybrids of (Phenylsulfonyl)furoxan and Anilinopyrimidine as Potent and Selective Epidermal Growth Factor Receptor Inhibitors for Intervention of Non-Small-Cell Lung Cancer, J. Med. Chem. 56 (2013) 4738-4748.

[28] M.M. Liu, X.Y. Chen, Y.Q. Huang, P. Feng, Y.L. Guo, G. Yang, Y. Chen, Hybrids of Phenylsulfonylfuroxan and Coumarin as Potent Antitumor Agents, J. Med. Chem. 57 (2014) 9343-9356.

[29] Y. Ai, F.H. Kang, Z.J. Huang, X.W. Xue, Y.S. Lai, S.X. Peng, J.D. Tian, Y.H. Zhang, Synthesis of CDDO−Amino Acid−Nitric Oxide Donor Trihybrids as Potential Antitumor Agents against Both Drug-Sensitive and DrugResistant Colon Cancer, J. Med. Chem. 58 (2015) 2452-2464.

[30] X.K. Gu, Z.J Huang, Z.G. Ren, X.B. Tang, R.F. Xue, X.J. Luo, S.X. Peng, H. Peng, B. Lu, J.D. Tian, Y.H. Zhang, Potent inhibition of nitric oxide-releasing bifendate derivatives against drug-resistant K562/A02 cells in vitro and in vivo, J. Med. Chem. 60 (2017) 928-940.

[31] J.C. Chen, T.Y. Wang, S.T. Xu, P.F. Zhang, A.J. Lin, L. Wu, H.Q. Yao, W.J. Xie, Z.Y. Zhu, J.Y. Xu, Discovery of novel antitumor nitric oxide-donating β-elemene hybrids through inhibiting the PI3K/Akt pathway, Eur. J. Med. Chem. 135 (2017) 414-423.

[32] N. Bao, J.F. Ou, M.Y. Xu, F.Q. Guan, W. Shi, J.B. Sun, L. Chen, Novel NO-releasing plumbagin derivatives: Design, synthesis and evaluation of

antiproliferative activity, Eur. J. Med. Chem. 137 (2017) 88-95.

[33] Y.L. Guo, Y.J. Wang, H.H. Li, K. Wang, Q. Wan, J. Li, Y.B. Zhou, Y. Chen, Novel nitric oxide donors of phenylsulfonylfuroxan and 3-benzyl coumarin derivatives as potent antitumor agents, ACS Med. Chem. Lett. 9 (2018) 502-506.

[34] N. Li, M.Y. Xu, N. Bao, W. Shi, Q.X. Li, X.W. Zhang, J.B. Sun, L. Chen, Discovery of novel NO-releasing celastrol derivatives with Hsp90 inhibition and cytotoxic activities, Eur. J. Med. Chem. 160 (2018) 1-8.

[35] J. L. Kelly, E.W. McLean, K.F. Willard, Synthesis of bis(arylsuh'onyl)furoxans from aryl nitromethyl sulfones, J Heterocycl. Chem. 14 (1977) 1415-1416.

[36] L. Yi, H.Y. Li, L. Sun, L.L. Liu, C.H. Zhang, Z. Xi, A highly sensitive fluorescence probe for fast thiol-quantification assay of glutathione reductase, Angew. Chem. Int. Ed. 48 (2009) 4034 -4037.

[37] Z.Y. Su, Z.Z. Yang, Y.Q. Xu, Y.B. Chen, Q. Yu, Apoptosis, autophagy, necroptosis, and cancer metastasis, Mol. Cancer. 14 (2015) 48.

[38] S. Elmore, Apoptosis: A review of programmed cell death, Toxicol. Pathol. 35 (2007) 495-516.

[39] D.R. Green, G. Kroemer, The pathophysiology of mitochondrial cell death, Science. 305 (2004) 626-629.

[40] P. Zhao, Y.N .Dou, L. Chen, L.H. Li, Z.F. Wei, J.T. Yu, X. Wu, Y. Dai, Y.F. Xia, SC-III3, a novel scopoletin derivative, induces autophagy of human hepatoma HepG2 cells through AMPK/mTOR signaling pathway by acting on mitochondria, Fitoterapia. 104 (2015) 31-40.

[41] H.U. Simon, A. Haj-Yehia, F. Levi-Schaffer, Role of reactive oxygen species (ROS) in apoptosis induction, Apoptosis, 5 (2000) 415-418.

[42] M.G. VanderHeiden, N.S. Chandel, E.K. Williamson, P.T. Schumacker, C.B. Thompson, Bcl-x (L) regulates the membrane potential and volume homeostasis of mitochondria, Cell. 91 (1997) 627-637.

[43] C.J. Sherr, Cancer cell cycles, Science. 274 (1996) 1672-1677.

Figure captions

Fig. 1. Scopoletin and representative scopoletin derivatives

Fig. 2. Phenylsulfonylfuroxan and phenylsulfonylfuroxan-based hybrids

Fig. 3. The design of novel scopoletin/phenylsulfonyfuroxan hybrids

Fig. 4. Compound **47** inhibited the colony formation of MDA-MB-231 cells. (A) Cells were incubated with DMSO or **47** (0.25, 0.5, and 1 μM) for 24 h and then cultured in a fresh medium for another 10 days, followed by staining with crystal violet. (B) The absorbance of crystal after staining at 590 nm (mean ± SD, n = 3). **P < 0.01, *P < 0.05

Fig. 5. Intracellular NO generated by the studied derivatives in MDA-MB-231 cells. (A) Cells were pretreated with DAF-FM DA and then incubated with scopoletin (10 μM) or **47** (1 and 10 μM) for 2.5 h, and then observed using a laser scanning confocal microscope (Olympus, Japan). (B) After cellular treatment with tested compounds (25 μM)) for 2.5 h, levels of intracellular NO were quantified using the total nitric oxide assay kit (mean ± SD, n = 3). (C) Cells were pretreated with hemoglobin (2.5, 5, 10, 20, and 40 μM) for 2 h and then incubated with **47** (4 μM) for another 48 h. The inhibition rates were measured by the MTT assay (mean ± SD, n = 3)

Fig. 6. Antiproliferative abilities of **51** and **52** and their equimolar mixture against MDA-MB-231 cells

Fig. 7. (A) MDA-MB-231 cells were separately treated with necrostain-1 (10 μM) and Z-VAD-FMK (20 μM) for 48 h, and the cell viability was measured by MTT method. (B) Cells were pretreated with necrostatin-1 or Z-VAD-FMK for 1 h and then

incubated with **47** (1.5, 2, and 3 μM) for another 48 h, and the inhibition rates were determined by MTT method (mean ± SD, n = 3). **P < 0.01, *P < 0.05

Fig. 8. Compound **47** induced the apoptosis of MDA-MB-231 cells. (A) Cells were treated with DMSO or **47** (0.5, 1, and 1.5 μM) for 24 h, and stained with Hoechst 33342. Cells were then observed under a fluorescent inverted microscope. (B) After treatment with DMSO or **47** (1, 1.5, 2, and 3 μM) for 24 h, cells were collected and sequentially stained with Annexin V and Propidium Iodide (PI), followed by flow cytometric analysis. (C) The percentages of early, late, and total apoptotic cells were calculated (mean ± SD, n = 3). **P < 0.01, *P < 0.05 vs. the negative control group.

Fig. 9. Compound **47** affected the mitochondrial membrane potential of MDA-MB-231 cells. (A) Cells were treated with **47** (1, 1.5, and 2 μM) and DMSO (control) for 18 h, harvested, and then stained with JC-1, followed by flow cytometric analysis. (B) The percentage of cells with green fluorescence or red fluorescence was determined (mean ± SD, n = 3), **P < 0.01, *P < 0.05 vs. the negative control group.

Fig. 10. Compound **47** induced ROS generation in MDA-MB-231 cells. (A) Cells were incubated with **47** (1, 1.5, and 2 μM) and DMSO (control) for 24 h, and then collected and stained with 2',7'-Dichlorofluorescin diacetate (DCFH-DA), followed by flow cytometric analysis. (D) The relative levels of fluorescent DCF were measured and plotted (mean ± SD, n = 3). **P < 0.01, *P < 0.05

Fig. 11. Compound **47** affected the expressions of mitochondrial apoptosis-related proteins in MDA-MB-231 cells. (A) Cells were incubated with DMSO or **47** (1.5, 3, and 6 μM) for 8 h, and levels of Bcl-2, Bax, Bad, cleaved-caspase-9,

cleaved-caspased-3, and cleaved-PARP were determined by western blotting. (B) Relative levels of mitochondrial apoptosis-related proteins were determined (mean ± SD, n = 3). **P < 0.01, *P < 0.05 vs. the negative control group

Fig. 12. Compound **47** blocked the cell cycle in the G2/M phase. (A) MDA-MB-231 cells were treated with **47** (1, 1.5, and 2 μM) or DMSO (control) for 24 h, and then collected, stained with PI, and analyzed by flow cytometric analysis. (B) The percentage of cells in each cell phase was determined (mean ± SD, n = 3). **P<0.01, *P<0.05 vs. the negative control group

- A series of phenylsulfonyfuroxan-based NO-releasing scopoletin derivatives were synthesized.
- The intracellular NO level was positively correlated with the antiproliferative ability.
- **47** releasing the highest amounts of NO possessed the best potency against MDA-MB-231 cells.

Declaration of interests

☒ The authors declare that they have no known competing financial interests or personal relationships that could have appeared to influence the work reported in this paper.

☐The authors declare the following financial interests/personal relationships which may be considered as potential competing interests: